Journal of Volcanology and Geothermal Research 276 (2014) 152–172

Contents lists available at ScienceDirect

Journal of Volcanology and Geothermal Research

journal homepage: www.elsevier.com/locate/jvolgeores

Eocene to Quaternary mafic-intermediate volcanism in San Luis Potosí, central Mexico: The transition from Farallon plate subduction to intra-plate continental magmatism

Alfredo Aguillón-Robles [a], Margarito Tristán-González [a], Gerardo de Jesús Aguirre-Díaz [b,*], Rubén A. López-Doncel [a], Hervé Bellon [c], Gilberto Martínez-Esparza [d]

[a] Instituto de Geología, UASLP, Av. Dr. Manuel Nava #5, Zona Universitaria, San Luis Potosí, S.L.P., Mexico
[b] Centro de Geociencias, Campus UNAM Juriquilla, Querétaro, Qro., Mexico
[c] UMR 6538, Domaines Océaniques, IUEM, Université de Bretagne Occidentale, 6, Av. Le Gorgeu, CS 93837, 29238, Cedex 3, France
[d] Posgrado en Geología Aplicada, DES Ingeniería, UASLP, Av. Dr. Manuel Nava #5, Zona Universitaria, San Luis Potosí, S.L.P., Mexico

ARTICLE INFO

Article history:
Received 13 June 2013
Accepted 26 February 2014
Available online 13 March 2014

Keywords:
Cordilleran calc-alkaline magmatism
Intra-plate alkaline volcanism
Cenozoic basalts and andesites
Central Mexico

ABSTRACT

The San Luis Potosí Volcanic Field (SLPVF) of central Mexico includes volcanic sequences of felsic, intermediate and basic compositions that were erupted as discrete episodes from the Eocene to the Pleistocene. Volcanism was dominated by widespread and voluminous rhyolitic ignimbrites of the mid-Tertiary Ignimbrite Flare-up. However, the complete volcanic history must consider basaltic and andesitic Eocene–Pleistocene volcanic successions that provide key evidence for understanding the geochemical evolution of the volcanism in the SLPVF during this time span. Five sequences are recognized according to their geochemical characteristics, each comprising a volcano-tectonic episode. The first episode comprises basaltic andesites and andesites erupted during three intervals, 45–42 Ma, 36–31 Ma, and 31–30 Ma. The oldest was derived from subduction magmatism, whereas the youngest has an intra-plate magmatic signature and this represents the transition from the end of a long lasting subduction regime of the Farallon plate to the initiation of intra-plate continental extension in the North American plate. The second episode, at 29.5–28 Ma, comprises a bimodal succession of high-silica rhyolites and alkaline basalts (hawaiites) that are interpreted as magmatism generated in an intra-plate continental extension regime during the Basin and Range faulting. The third episode, at 21 Ma, is characterized by trachybasalts and trachyandesites that represent mantle basaltic melts that were contaminated through assimilation of the lower crust during advanced stage of intra-plate extension that started at Oligocene. The fourth episode includes 12 Ma alkaline basalts and andesites that were erupted from fissures. These mantle derived magmas evolved to andesites by crustal anatexis and crystal fractionation within a continued, extensional, intra-plate regime. Lastly, the fifth episode comprises 5.0 to 0.6 Ma alkaline basalts (basanites) containing mantle xenoliths, that were erupted from maars and tuff cones, which are the youngest manifestations of mantle-derived intra-plate extensional events. Based upon this volcanic record, the last subduction manifestations of the extinct Farallon plate occurred at about 42 Ma, this was followed by a transition to intra-plate magmatism between 42 and 31 Ma, and an extensional, intra-plate tectonic setting from 31 Ma to almost Present.

1. Introduction

The San Luis Potosí Volcanic Field (SLPVF), located in the Mesa Central of Mexico (Fig. 1), includes intermediate-mafic volcanism ranging in age from Eocene to Quaternary. The Sierra Madre Occidental (SMO) is an Eocene–Miocene volcanic province, which consists of a lower sequence of Eocene orogenic-type volcanic rocks dominated by intermediate lavas, a middle sequence of rhyolitic volcanic rocks dominated by Oligo-Miocene ignimbrites, and an upper sequence of mafic lavas, mostly early Miocene in age and dominated by basaltic andesites and alkaline basalts (McDowell and Clabaugh, 1979; Damon et al., 1981; Aguirre-Díaz and McDowell, 1991, 1993; Aguirre-Díaz et al., 2008; Tristán-González et al., 2009a). Volcanism posterior to the SMO, in central-northern Mexico, and particularly in SLPVF, was dominated by basaltic andesites and alkaline basalts widely distributed and preserved as small patches in the region that have ages ranging from middle Miocene to Quaternary (Tristán-González et al., 2009a).

Based upon previous works, the stratigraphy of the SLPVF includes 44 Ma andesites of Casita Blanca Formation, 32–27 Ma rhyolitic and

* Corresponding author at: Centro de Geociencias, UNAM, Blvd. Juriquilla 3001, Col. Campus UNAM, Juriquilla, Querétaro, Qro. CP 76230, México.
E-mail addresses: aaguillonr@uaslp.mx (A. Aguillón-Robles), mtristan@uaslp.mx (M. Tristán-González), ger@geociencias.unam.mx (G. de Jesús Aguirre-Díaz), rlopez@uaslp.mx (R.A. López-Doncel), Herve.Bellon@univ-brest.fr (H. Bellon), esparzamtz@hotmail.com (G. Martínez-Esparza).

http://dx.doi.org/10.1016/j.jvolgeores.2014.02.019
0377-0273/

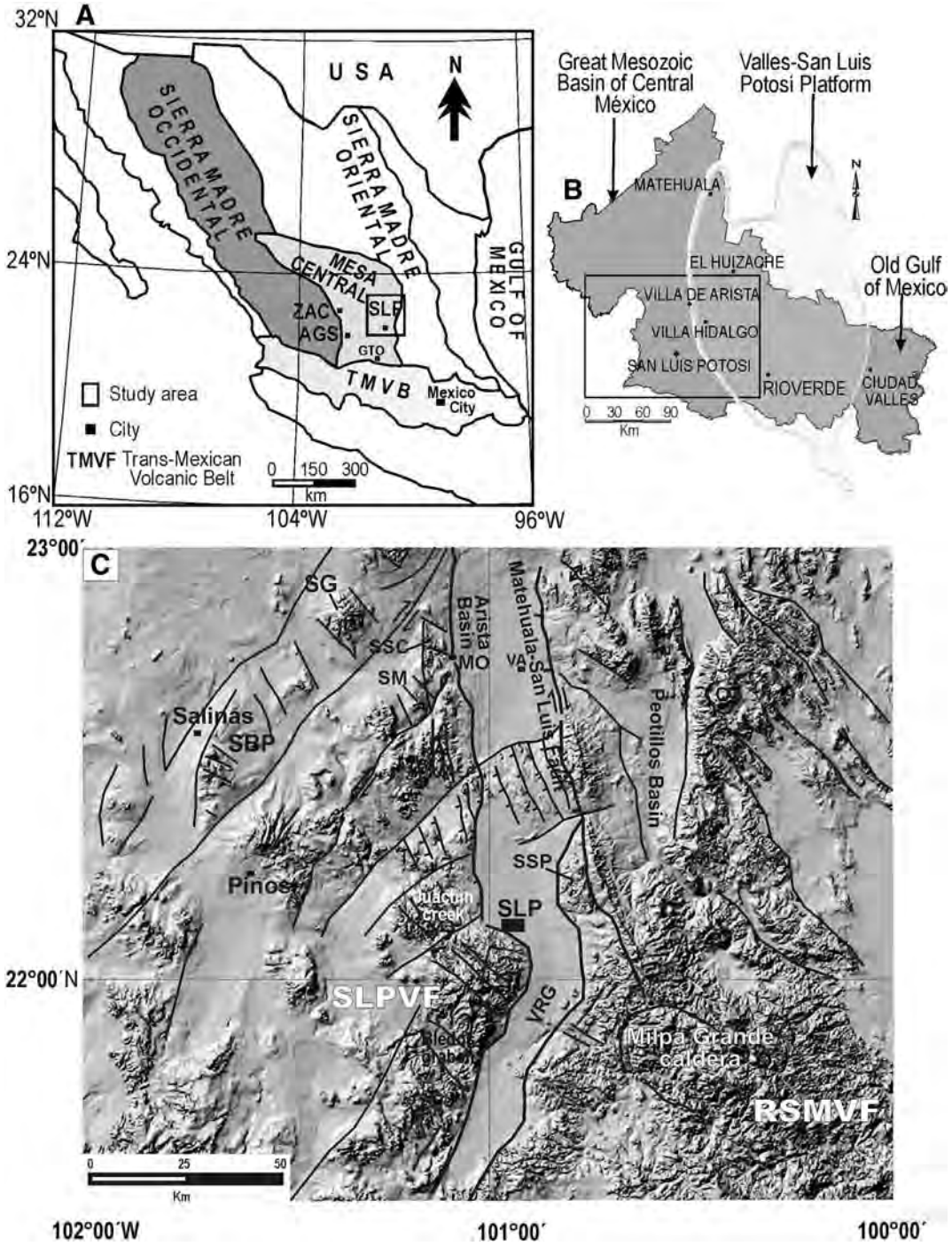

Fig. 1. Location of San Luis Potosí (SLPVF) and Río Santa María volcanic fields (RSMVF). A) Spatial relationship with the main geological provinces of northern Mexico; ZAC, Zacatecas city; AGS, Aguascalientes city; GTO, Guanajuato city; SLP, San Luis Potosí, city (modified after Tristán-González et al., 2009b). B) Location of the main volcano-tectonic features of the San Luis Potosí State. C) Digital elevation model showing the main tectonic structures in the SLPVF and surrounding area. RSMVF, Río Santa María Volcanic Field; SG, Sierra Guanamé; SSC, Sierra Santa Catarina; SM, Sierra Las Minas; SBP, Sierra La Ballena–Peñón Blanco; SSP, Sierra San Pedro, MO, Moctezuma; VA, Villa Arista; VRG, Villa de Reyes Graben.

dacitic ignimbrites and lava domes with sparse 30 Ma andesites, and a bimodal, 28 Ma succession represented by the widespread Panalillo rhyolitic ignimbrite and La Placa basalt (Labarthe-Hernández et al., 1982; Idier, 2003; Rodríguez-Ríos and Torres-Aguilera, 2009; Tristán-González et al., 2009a). The last volcanic stages in the SLPVF consists of Middle Miocene and Plio-Pleistocene alkaline basalts including basanites and trachybasalts (Luhr et al., 1995; Martínez-Esparza, 2004). Eocene–Oligocene volcanism in the Mesa Central was mostly controlled by NW–SE normal faults, whereas Quaternary volcanism was controlled by E–W and N–S normal faults (Tristán-González, 2008; Tristán-González et al., 2009b).

It is well documented that felsic volcanism predominates in the SLPVF, where it is represented by mid-Tertiary dacitic-rhyolitic lavas and high-silica rhyolitic ignimbrites (Labarthe-Hernández et al., 1982; Aguirre-Díaz et al., 2008; Aguillón-Robles et al., 2009). In contrast, the intermediate-mafic volcanic rocks are less well known and less studied than the voluminous felsic volcanic rocks. However, despite its relatively smaller volume, the intermediate-mafic volcanic rocks are

key representative products of tectonic regime changes that occurred in central Mexico from Eocene to Pleistocene.

We have grouped intermediate to mafic volcanism of the SLPVF into five major episodes, 1) Eocene andesites, 2) Oligocene basaltic andesites and andesites, 3) Early Miocene basalts and trachytes, 4) Middle Miocene basalts, and 5) Plio-Pleistocene basalts. In this manuscript we describe and interpret the geochemical characteristics of these five volcanic episodes, in order to establish the tectonic regime for each and the geochemical evolution of intermediate to mafic magmatism from the Eocene to Quaternary in the SLPVF.

2. Geological setting

The oldest rocks known in the Mesa Central are Triassic marine sedimentary rocks with a low grade regional metamorphism that mark the continental margin at that time and form the basement for the region (Barboza-Gudiño et al., 1998; Hoppe et al., 2002; Barboza-Gudiño et al., 2010). Unconformably overlying the Triassic basement rocks are Jurassic volcano-sedimentary rocks that include basaltic pillow lavas, andesites, and marine and continental sedimentary rocks, which have been interpreted as the Guerrero accreted terrane (Campa-Uganda and Coney, 1983; Centeno-García and Silva-Romo, 1997; Zavala-Monsiváis et al., 2012). Marine sedimentary conditions persisted throughout the Mesa Central from the Oxfordian to the end of the Cretaceous. During this interval three lithostratigraphic sequences were deposited related to two paleogeographic features (Fig. 1). The first feature, referred to as the Valles–San Luis Potosi platform, comprises a marine carbonated sequence (Carrillo-Bravo, 1971); and the second feature, known as the Great Mesozoic Basin of Central Mexico (GMBCM; Carrillo-Bravo, 1982), which covers a large portion of the central-eastern Mesa Central, comprises a marine sedimentary sequence that ranges in age from Late Triassic to Late Cretaceous. These Mesozoic sequences were strongly deformed by an eastward directed shortening event during the Laramide orogeny at K/T time (Guzmán and De Cserna, 1963; Eguiluz-de Antuñano et al., 2000; Tristán-González et al., 2009b).

Overlying and in angular unconformity with the Mesozoic rocks is a Paleocene–Eocene sedimentary sequence consisting mostly of continental clastic deposits (red beds; Fig. 2). Intercalated andesitic lavas in the clastic sequence are dated at 49–44 Ma (Aranda-Gómez and McDowell, 1998; Tristán-González et al., 2008; Fig. 2). Covering the lava is a thick Oligocene volcanic succession that was emplaced as two events: the first, at 32–31 Ma, includes dacitic lavas in the form of domes, and the second event at 31–28 Ma, consists of voluminous rhyolitic ignimbrites and rhyolitic domes (Labarthe-Hernández et al., 1982; Fig. 2). Overlying the felsic sequence are basaltic andesites and alkaline basalts, which were erupted during the early and middle Miocene (22 and 12 Ma) and Plio-Pleistocene (5–0.6 Ma; Fig. 2).

Volcanism of intermediate composition in the SLPVF started in the middle Eocene and is represented by the Casita Blanca andesite unit (Fig. 2). Several ages are reported for the andesites, giving a range of 45.5–42.5 Ma and 36.4–31.2 Ma (Tristán-González et al., 2009a; Table 1). The andesitic lavas erupted from a central vent or fissures (dikes) to form fine-grained, low aspect ratio lava flows. In a regional

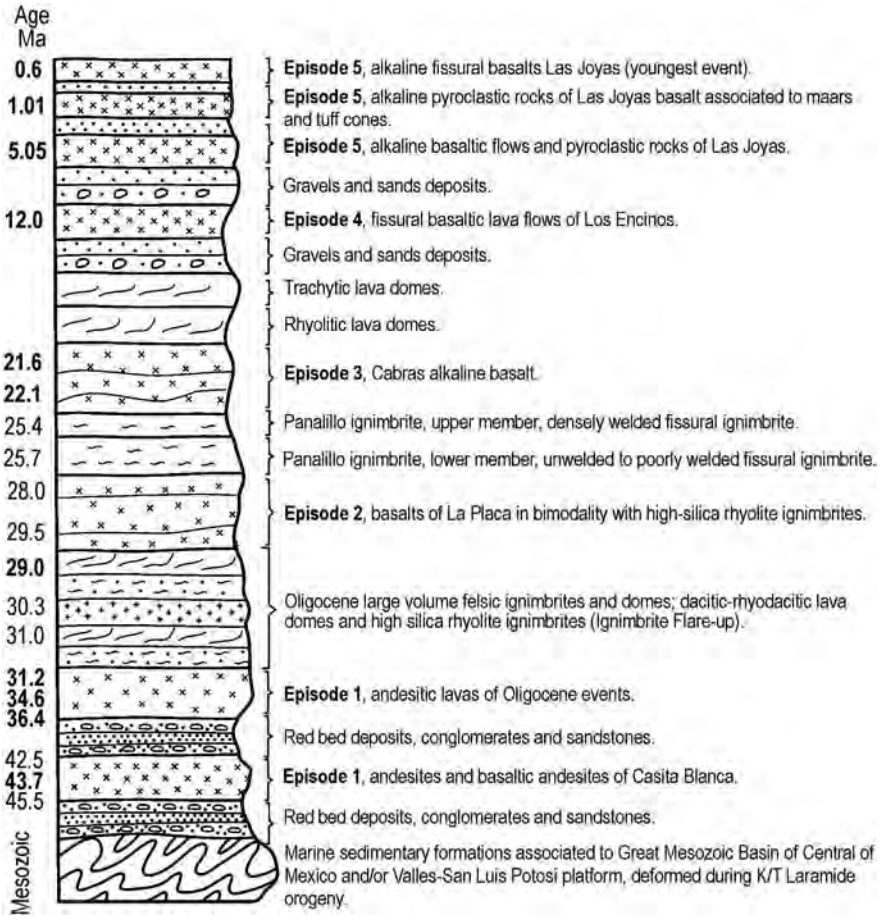

Fig. 2. Composite stratigraphic column for the SLPVF showing the main lithostratigraphic units described in text and the five volcanic episodes of intermediate to mafic volcanism described in this work. Ages in bold font are new and from this study (Table 2), other ages are from published works (Table 1).

Table 1
K-Ar ages of mafic volcanism in the Sierra Madre Occidental Province.

Sample	Rock type	Age ± 1σ (Ma)	Region	Method (material used)	Reference
SLP01-25	Basalt	1.5 ± 0.8	AVC	K-Ar (wr)	Tristán-González et al., (2009b)
RK 24	Basalt	12.4 ± 0.4	Dgo	K–Ar (a)	McDowell and Keiser (1977)
R-14	Basalt	22.4 ± 0.4	Dgo	K–Ar (wr)	Aguirre-Díaz and McDowell (1991)
SLP00-14	Basalt	26.9 ± 0.6	SSMVC	K–Ar (wr)	Tristán-González et al. (2009a)
JL-BR-SI	Basalt	29.5 ± 0.6	Dgo	K–Ar (wr)	McDowell and Keiser (1977)
SLP01-35	Andesite	30.5 ± 0.7	VHVC	K–Ar (wr)	Tristán-González et al. (2009a)
SLP03-01	Andesite	31.6 ± 0.7	VHVC	K–Ar (wr)	Tristán-González et al. (2009a)
SLP99-03	Andesite	31.6 ± 0.7	RSMVC	K–Ar (wr)	Tristán-González et al. (2009a)
SLP03-02	Andesite	31.9 ± 0.7	RSMVC	K–Ar (wr)	Tristán-González et al. (2009a)
SLP0206	Andesite	31.2 ± 0.7	AVC	K–Ar (wr)	Idier (2003)
SL-46	Andesite	40.3 ± 1.0	Dgo	K–Ar (pl)	Aguirre-Díaz and McDowell (1991)
SLP01-06	Andesite	42.5 ± 1.0	RSMVC	K–Ar (wr)	Tristán-González et al. (2009a)
Tc	Andesite	44.1 ± 2.2	AVC	K–Ar (wr)	Labarthe-Hernández et al. (1982)
01-33	Andesite	44.4 ± 1.0	AVC	K–Ar (wr)	Tristán-González et al. (2009b)
01-31	Andesite	45.5 ± 1.1	AVC	K–Ar (wr)	Tristán-González et al. (2009a)
Na-13	Andesite	48.8 ± 3.0	Dgo	K–Ar (pl)	Aguirre-Díaz and McDowell (1991)
CG	Andesite	49.3 ± 1.0	Gto	K–Ar (wr)	Aranda-Gómez and McDowell (1998)
RK 18	Andesite	51.6 ± 1.3	Dgo	K–Ar (pl)	McDowell and Keiser (1977)

Dgo, Durango State; SSMVC, Sierra San Miguelito volcanic complex; RSMVC, Río Santa María volcanic complex; VHVC, Villa Hidalgo volcanic complex; AVC, Ahualulco volcanic complex; Gto, Guanajuato State. Material used: a, amphibole; wr, whole rock; pl, plagioclase.

context, these andesitic flows are equivalent to Eocene andesites reported in several localities throughout the SMO volcanic province, such as andesitic units in the states of Zacatecas and Sinaloa (Clark et al., 1979), the Antigua andesite of Durango State (McDowell and Keiser, 1977), Pedriceñas and Playas andesite also in the State of Durango (Aguirre-Díaz and McDowell, 1991), and andesitic lavas intercalated with red conglomerates of Zacatecas and Guanajuato (Edwards, 1955; Aranda-Gómez and McDowell, 1998). Therefore, andesitic volcanism was widespread during the Eocene in northern Mexico (Aguirre-Díaz and McDowell, 1991).

The principal volcanic event of the SLPVF occurred at 31–29 Ma and is represented by large volume ignimbrites, all high-silica rhyolites (Labarthe-Hernández et al., 1982; Tristán-González et al., 2009a; Tristán-González et al., 2009b). Originally, it was proposed that the ignimbrites were derived from the Milpa Grande caldera (Labarthe-Hernández et al., 1989). However, recent studies argue that some of these as well as other younger ignimbrites of the region were associated with Basin and Range fault systems (Aguirre-Díaz and Labarthe-Hernández, 2003; Torres-Hernández et al., 2006; Tristán-González et al., 2006, 2008; Aguirre-Díaz et al., 2008). Lavas of basic to intermediate composition and of a similar age are distributed, albeit scarcely, in the SLPVF (Tristán-González et al., 2009a; Fig. 2; Table 2).

At 31.5 Ma, NNE to NW chain lava domes of rhyodacitic composition were emplaced in the east and southeast of the SLPVF. Subsequent to the emplacement of these domes, the Villa de Reyes graben, a NW to NNE oriented structure (Fig. 1), was formed. The last pyroclastic eruptions were fed from fissures associated with the graben's master faults (Labarthe-Hernández et al., 1982; Tristán-González, 1986; Tristán-González et al., 2009a, 2009b). Contemporaneously, there were sparse eruptions of andesitic and basic lava flows, apparently also controlled by the extension faults of SLPVF (Tristán-González et al., 2008, 2009b).

Immediately following the 31.5 Ma rhyodacitic, effusive volcanism, there was a massive eruption of ignimbrite-forming pyroclastic flows and lava domes, all high-silica rhyolites. This major silicic event was fed from fissures related to main normal fault systems generally oriented NW (Aguirre-Díaz and Labarthe-Hernández, 2003; Torres-Hernández et al., 2006; Aguirre-Díaz et al., 2008; Tristán-González et al., 2009b).

Table 2
New K–Ar ages of andesitic and basaltic volcanic rocks from the SLPVF.

Samples	Rock type	Geologic unit	Age ± 1σ	Longitude (W)	Latitude (N)	Fraction	$^{40}Ar_R$ (10^{-7} cm^3/g)	$^{40}Ar_R$ (%)	K_2O (wt.%)	Weight (g)	Ref. lab
TG 49	BSN	Qbj	0.6 ± 0.06	100.6296	22.2760	WR	0.41	10.0	2.15	1.0056	6479
TG 43	A	Qbj	1.01 ± 0.10	100.6594	22.5572	WR	0.75	12	2.30	1.0035	6470
GME03-44	BSN	Qbj	5.05 ± 0.14	100.7273	22.4075	WR	1.60	40.2	1.92	1.0169	6471
RV08	B	Tle	12.0 ± 0.3	100.0985	22.0066	WR	4.30	51.3	1.11	0.363	7079
SLP99-02	B	Tbc	21.5 ± 0.5	101.4815	22.3675	WR	8.51	74.1	1.22	0.5074	5126
SLP03-03	BTA	Tbc	21.6 ± 0.5	101.1772	21.9114	WR	21.48	57.9	3.14	1.000	6443
SLP06-01	BTA	Tbc	22.1 ± 0.5	101.2993	21.8723	WR	19.71	71.8	2.75	0.3624	7076
SLP00-02	A	Tbp	28.0 ± 0.6	101.1519	22.1406	WR	26.50	55.5	2.91	0.5079	5496
SLP03-05	A	Tbp	29.0 ± 0.7	101.0842	21.8105	WR	20.03	76.8	2.18	1.0087	6444
TG 52	A	Tbp	29.5 ± 0.7	100.8861	21.7733	WR	12.80	77.9	1.34	1.0124	6497
SLP02-06	A	Tcb	31.2 ± 0.7	101.2247	22.4425	WR	23.96	71.7	2.36	0.6000	6345
GME0336	A	Tcb	34.6 ± 0.8	101.2643	22.5108	WR	25.76	71.2	2.29	1.0050	6448
SLP02-17	A	Tcb	36.4 ± 1.4	101.1337	22.6026	WR	26.11	69.4	2.20	1.0016	6331
SLP 01-06	BA	Tcb	42.5 ± 1.0	100.7719	22.2258	WR	20.80	72.2	1.50	0.6140	6308
SLP02-14	BA	Tcb	43.7 ± 1.0	101.1749	22.4982	WR	31.82	77.5	2.22	0.6043	6320

Rock type: BSN, basanite; B, basalt; BA, basaltic-andesite; BTA, basaltic trachy-andesite; A, andesite. Geologic unit: volcanic stratigraphy reported by Labarthe-Hernández et al. (1982) and Tristán-González et al. (2009a). Age ± 1σ; calculated with the equation proposed by Cox and Dalrymple (1967), for samples older than 5 Ma, and the equation given by Mahood and Drake (1982) for samples younger than 5 Ma. Fraction: WR, whole rock. K_2O (wt.%): weight per cent of potassium. Ref. lab.: Reference given by the Laboratory of Geochronology at Université de Bretagne Occidentale.

Basin and Range normal faulting was active by 32 Ma in the SLPVF, and it was apparently synchronous with Oligocene silicic volcanism (Tristán-González et al., 2009b). This syn-extensional silicic volcanism continued through to 25 Ma, when a major ignimbrite, the Panalillo Rhyolite, was emplaced (Labarthe-Hernández et al., 1982; Tristán-González et al., 2008, 2009b; Fig. 2). Initially, it was proposed that this widespread unit was emplaced after fault-bounded depressions had formed as the ignimbrite occurred within them (Labarthe-Hernández et al., 1982), but new studies demonstrate that the Panalillo ignimbrite was erupted and emplaced synchronously with graben development and that the eruptions were fed from multiple fissure vents (Aguirre-Díaz and Labarthe-Hernández, 2003; Torres-Hernández et al., 2006; Tristán-González et al., 2006; Aguirre-Díaz et al., 2008; Tristán-González et al., 2008, 2009b). Based on an age of ca. 28 Ma obtained for the lower member of the Panalillo ignimbrite (Tristán-González et al., 2009a), and that it occupies a stratigraphic position immediately above the La Placa basalt, it has been proposed that volcanism was bimodal at this time (Rodríguez-Ríos and Torres-Aguilera, 2009; Tristán-González et al., 2009a, 2009b). However, the Panalillo ignimbrite yielded ages that range between 28 Ma and 25.4 Ma (Tristán-González et al., 2009a), which indicates several volcanic phases for the formation of Panalillo ignimbrite. Bimodality also took place between La Placa basalt and rhyolitic lava domes of about 29 Ma in the SLPVF (Aguillón-Robles et al., 2009). Faulting continued after emplacement of the Panalillo ignimbrite as it is generally faulted and tilted.

Early Miocene basaltic lavas were erupted just after the last phases of the Panalillo ignimbrite (Tristán-González et al., 2009a, 2009b; Rodríguez-Ríos and Torres-Aguilera, 2009; Fig. 2). The basalts have an alkalic affinity and are inferred as been generated in an intra-plate regime during an intense extensional period of the Basin and Range (Tristán-González et al., 2009b). Similar age alkaline basalts are reported in several localities in the SMO, such as Metates, Durango (McDowell and Clabaugh, 1979), Nazas, Durango (Aguirre-Díaz and McDowell, 1993), and central Chihuahua (McDowell and Keiser, 1977; Cameron et al., 1989). Aguirre-Díaz et al. (2008) group them all in the Miocene Mafic Lava suite of the Sierra Madre Occidental, which includes basaltic andesites and alkali basalts of early Miocene age (24–18 Ma) that occurred throughout the SMO generally overlying the rhyolitic ignimbrites.

Fissure-fed, alkalic basalts were erupted during the middle Miocene in the SLPVF. These lavas were first reported as the Los Encinos volcanic field (Luhr et al., 1995). This alkalic mafic activity continued during the Pliocene and through the Pleistocene in the form of phreatomagmatic eruptions from maars or fissures related to major faults (Tristán-González et al., 2009b). The juvenile scoria and lavas have a basanite composition (Aranda-Gómez et al., 1993). The near vent products contain xenoliths from the peridotitic mantle and from the Precambrian lower crust (Aranda-Gómez et al., 1993, 2005). The crustal granulite xenoliths yielded a Sm–Nd model age of 1248 ± 69 Ma (Schaaf et al., 1994).

3. Tectonic setting

The SLPVF volcanic sequence rests on Mesozoic marine sediments deformed during the Laramide orogeny. Engebretson et al. (1984) and Livaccari et al. (1981) proposed that this orogeny resulted from flat subduction due to the relatively fast subduction of the extinct Farallon plate throughout the North American continental margin. Flat subduction caused a regional uplift along the fore arc, suppression of arc magmatism and compressional deformation in the continental plate (Humphreys, 2009). Molnar and Atwater (1978) proposed that deformation throughout the North American continental margin was related to long term subduction of relatively young lithosphere of the Farallon–Kula plates. Subduction of relatively young oceanic lithosphere (<50 Ma) is associated with cordilleran tectonics and the formation of high ranges, zones of extensive deformation, inverse faults and normal cortical shortening to the axis of the arc (Engebretson et al., 1984). The laramidic arc of Mexico produced substantial volumes of plutonic and volcanic rocks, which were grouped in the Lower Volcanic Group of the SMO (McDowell and Keiser, 1977; McDowell et al., 2001; Aguirre-Díaz et al., 2008). The plutonic rocks range from diorites to alkaline granite and the volcanic rocks from andesite to rhyolite, with a predominance of andesite (Nemeth, 1976; Henry and Fredrikson, 1987; McDowell et al., 1989; Roldán-Quintana, 1991; Albretch and Goldstein, 2000; McDowell et al., 2001). After the event of Laramide shortening in the western and central part of Mexico, a widespread extensional tectonic event (Basin and Range) took place in the early Oligocene, which generated sets of contemporaneous normal faults and syn-tectonic volcanic events that continued through the Oligocene–Miocene time (Henry and Aranda-Gómez, 1992; Aguirre-Díaz and McDowell, 1993; Stewart, 1998; Tristán-González et al., 2009b). Damon et al. (1981) related the generation of mid-Tertiary volcanism of western Mexico to a progressive change of dip of the subducted Farallon plate that caused an eastward migration of magmatic arc, reaching as far as 1000 km of the paleotrench. Damon et al. (1983) mention that the Lower Volcanic Group ranges in age between 90 and 40 Ma, with the youngest rocks located at the eastern margin of the SMO. It has also been suggested that volcanism was simultaneous across that arc, at least during the Eocene (Aguirre-Díaz and McDowell, 1991; Tristán-González et al., 2009b). Along with calc-alkaline arc volcanism there are Eocene andesites and Miocene alkaline basalts with intra-plate signatures in northwestern and central Mexico (Cameron et al., 1980; Cameron and Hanson, 1982; Aguirre-Díaz and McDowell, 1993; Bryan et al., 2008; Aguillón-Robles et al., 2009). The early Miocene basaltic volcanism was related to extension during Basin and Range intra-plate volcanism (Aguirre-Díaz and McDowell, 1993; Tristán-González et al., 2009b), and the Plio-Quaternary volcanism to intra-plate mantle-derived magmatism (Aranda-Gómez et al., 2005).

4. K–Ar geochronology

Isotopic ages of selected volcanic units were determined using the K–Ar method at the Geochronology Laboratory of the Université de Bretagne Occidental (UBO) at Brest, France. After crushing and sieving the rock to a size fraction between 0.3 to 0.15 mm, the sample was washed with distilled water and then saved for analytical purposes in two aliquots, one aliquot was reduced to powder (diameter < 60 μm) in an agate grinder for K analyses by atomic absorption spectrometer (AAS) after a chemical attack with hydrofluoric acid, and from the second aliquot, 0.3 to 0.15 mm grains were used for the isotopic analysis of Ar. Argon extraction was done under high vacuum condition by induction heating in a molybdenum crucible. The extracted gases were purified in a line of two titanium sponge furnaces and two Al–Zr SAES getters for noble gas cleaning. The isotopic argon composition and radiogenic ^{40}Ar were measured using a stainless steel mass spectrometer with 180° geometry, equipped with an amplifier Keithley 642. The isotopic dilution method was applied using a spike of ^{38}Ar that was implanted as ion in a small aluminum target. Details of the method are described in Bellon et al. (1981).

The new isotopic ages are shown in Table 2. The ages were calculated using the constants recommended by Steiger and Jäger (1977), and the incertitude of the error of ±1σ was calculated using the equation of Cox and Dalrymple (1967) for samples older than 5 Ma. The equation of Mahood and Drake (1982) was used for samples younger than 5 Ma.

The new K–Ar ages are compared with previous ages reported for the SLPVF in Table 2. The Casita Blanca andesite yielded three events, firstly at 43.7 Ma, the second event at 34.6 Ma, and the last one at 31.2 Ma (Fig. 2). Both agree with stratigraphy and indicate that Casita Blanca andesite volcanic eruptions in different times during the Eocene to early Oligocene. La Placa basalt yielded 29.5 to 28.0 Ma. The Cabras basalt yielded ages of 22.1 to 21.5 Ma, all within analytical error. Only one sample from the Los Encinos basalt was dated, yielding an age of 12.0 ± 0.3 Ma, and it is interpreted as corresponding to a young event

from the Los Encinos volcanic field (Luhr et al., 1995; Aranda-Gómez et al., 2005). The Las Joyas basalt returned three ages, one at 5.05 ± 0.14 and the others at 1.01 ± 0.10 and 0.6 ± 0.06; this indicates that there were two eruptive events associated with Las Joyas volcanism, one around 5 Ma and the other of Pleistocene age (Tristán-González et al., 2009a).

5. Andesitic and basaltic volcano-tectonic episodes in the SLPVF

Andesitic and basaltic volcanism in the SLPVF is grouped into five different episodes according to age and composition, each representing a volcano-tectonic event and having distinct petrologic characteristics. Episode 1 includes Late to Middle Eocene andesitic lavas in which Casita Blanca andesite is the principal unit. It forms the basal part of the SMO volcanic sequence in the SLPVF. Episode 2 includes Late Oligocene basalts of La Placa unit and Oligocene rhyolites, defining a bimodal succession. Episode 3 includes the Early Miocene Cabras alkalic basalts. Episode 4 is represented by the Middle Miocene Los Encinos alkalic basalts, and Episode 5 by the Plio-Pleistocene Las Joyas alkali basalts.

5.1. Episode 1

It includes three andesitic units occurring at 45–42 Ma, 36–34 Ma, and at 31 Ma. The oldest group corresponds to Casita Blanca andesite, with ages between 45.5 ± 1.0 and 42.5 ± 1.0 Ma (Tables 1 and 2) and includes the 45.5 Ma andesite reported by Tristán-González et al.

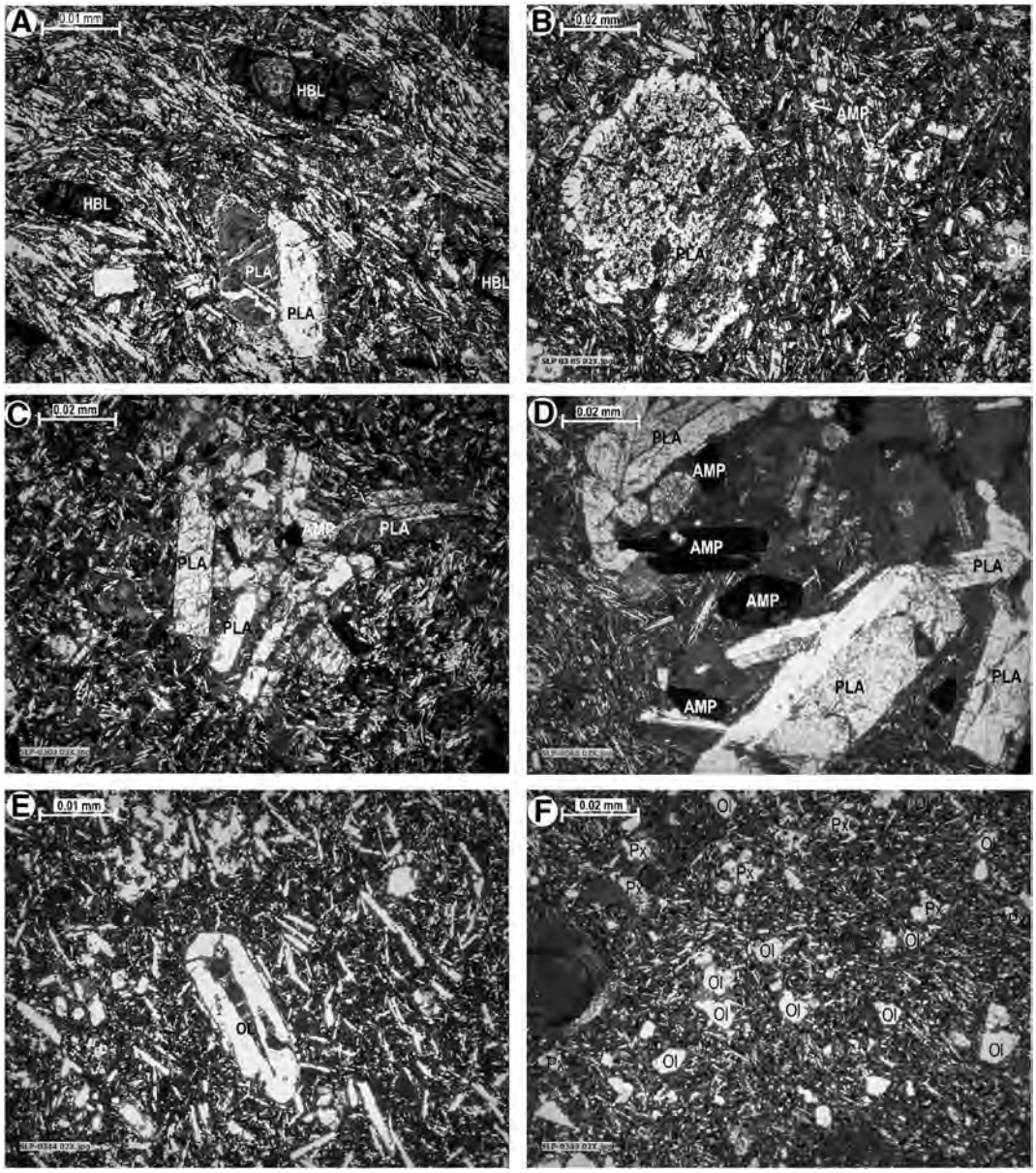

Fig. 3. Photomicrographs showing the microscopic textures of representative samples of each volcanic episode described in main text. All using polarized light. Scale is shown in each photo. A) Casita Blanca Andesite (Episode 1), showing a trachytic texture with euhedral to subhedral porphyritic crystals, oscillatory zoned plagioclase (PLA), oxidized hornblende (HBL), and a groundmass with intergranular plagioclase microlaths. B) La Placa Basalt (Episode 2), showing a hypocrystalline, hypidiomorphic texture, with xenocrysts of feldspar with reaction coronas, and a groundmass of interstitial plagioclase and olivine (OL). C) Cabras Basalt (Episode 3) showing a holocrystalline, inequigranular and glomero-porphyritic texture, with phenocrysts of plagioclase (PLG), hornblende (AMP), and a groundmass of interstitial plagioclase, olivine and augite. D) Los Encinos Basalt (Episode 4), showing a porphyritic texture, with phenocrysts of plagioclase (PLA) and altered hornblende (AMP), and a groundmass of fine grained plagioclase, augite and glass. E) Las Joyas Basalt (Episode 5) 5 Ma lava, with a microporphyritic texture containing euhedral olivine (OL) with iddingsitized rims, small laths of plagioclase and titano-augite. F) Las Joyas Basalt (Episode 5) 0.6 Ma scoriae, with a hypocrystalline- trachytic texture, containing subhedral olivine (Ol), titano-augite (Px), and a groundmass composed of microlitic plagioclase and glass.

Table 3a
Major and trace element analyses of andesitic and basaltic volcanic rocks from the SLPVF. Episode 1, Casita Blanca andesite.

Sample	SLP0106	GME0332	GME0333	GME0335	GME0336	GME0337	GME0338	GME0339	SLP0206
Rock type	BA	A	A	A	A	A	A	BA	A
VU	Tcb	Tcb	Tcb	Tcb	Tcb	Tcb	Tcb	Tcb	Tcb
Major elements (wt.%)									
SiO_2	52.90	59.00	59.90	59.00	58.00	61.00	56.80	54.80	58.20
TiO_2	1.20	1.29	1.13	1.29	1.27	1.13	1.35	1.40	1.21
Al_2O_3	16.80	15.30	15.85	15.30	15.65	15.60	16.25	16.30	16.20
Fe_2O_3	8.54	6.45	4.94	6.45	7.40	6.42	7.25	8.04	5.90
MnO	0.13	0.10	0.06	0.10	0.13	0.10	0.30	0.12	0.04
MgO	5.46	4.06	3.60	4.12	3.95	3.36	4.40	5.45	3.40
CaO	7.40	5.92	5.54	5.78	5.65	4.72	6.25	6.88	5.54
Na_2O	3.30	3.29	3.39	3.39	2.80	3.35	3.20	3.15	3.52
K_2O	1.54	1.62	2.14	1.89	2.12	1.54	1.56	1.84	2.20
P_2O_5	0.28	0.48	0.38	0.46	0.39	0.36	0.40	0.41	0.43
LOI	1.92	2.01	2.53	1.38	2.02	2.12	1.82	1.93	3.01
Total	99.47	99.52	99.46	99.16	99.38	99.7	99.58	100.32	99.65
CIPW normative minerals (calculated with the SINCLAS program)									
qz	4.522	16.578	16.500	15.243	16.136	20.995	12.875	7.693	13.888
or	9.378	9.857	13.084	11.465	12.930	9.361	9.473	11.110	13.504
ab	28.787	28.660	29.684	29.448	24.446	29.159	27.822	27.23	30.928
an	27.292	22.854	22.466	21.513	24.633	21.674	26.068	25.436	22.750
ne	–	–	–	–	–	–	–	–	–
di	6.939	3.306	2.688	3.847	1.331	–	2.485	5.336	2.284
hy	15.293	11.224	9.355	10.957	12.717	11.116	13.501	14.93	9.545
ol	–	–	–	–	–	–	–	–	–
Trace elements (ppm)									
Rb	47.50	84.00	59.00	104.00	79.00	91.00	50.00	50.00	58.50
Ba	460.00	920.00	812.00	965.00	880.00	1050.00	915.00	685.00	840.00
Th	3.70	7.70	6.30	7.50	9.00	11.20	7.60	6.10	6.60
Nb	11.00	13.70	11.40	13.50	16.50	14.80	14.90	15.40	12.50
La	22.00	50.50	44.50	50.50	43.00	46.00	38.00	33.00	46.00
Ce	43.00	108.00	94.00	104.00	90.00	95.00	76.00	66.00	100.00
Sr	472.00	920.00	1030.00	910.00	416.00	408.00	500.00	465.00	1080.00
Nd	26.00	55.00	49.00	54.00	45.00	46.00	40.50	33.50	52.00
Sm	5.60	10.10	8.60	9.70	9.00	8.60	7.60	7.30	8.80
Zr	145.00	304.00	230.00	310.00	330.00	318.00	291.00	250.00	276.00
Eu	1.58	2.25	2.08	2.20	1.89	1.72	1.80	1.78	2.16
Gd	5.50	7.20	6.35	7.00	7.00	6.65	6.70	6.50	6.10
Dy	4.50	4.90	4.20	4.75	5.30	4.90	5.00	5.05	4.25
Y	26.00	25.50	21.80	26.00	29.00	27.50	28.50	28.50	22.20
Er	2.45	2.40	2.00	2.45	2.70	2.60	2.70	2.70	2.00
Yb	2.25	2.03	1.67	2.04	2.45	2.22	2.27	2.33	1.70
Sc	23.50	13.50	14.00	14.00	16.00	15.00	18.00	21.00	15.20
V	235.00	120.00	125.00	116.00	125.00	122.00	152.00	174.00	124.00
Cr	280.00	130.00	118.00	125.00	125.00	110.00	130.00	180.00	124.00
Co	29.00	18.00	15.00	18.00	20.00	16.00	22.00	27.00	15.00
Ni	80.00	64.00	51.00	46.00	65.00	30.00	56.00	93.00	39.00
A.I.	2.540	1.680	1.770	1.810	1.770	1.500	1.870	2.310	2.000
Mg#	66.912	67.522	71.244	68.137	63.658	63.658	66.263	68.577	66.100
DI	42.687	55.095	59.268	56.156	53.512	59.515	50.170	46.033	58.320

Sample	SLP0214	SLP0217	B35	Mean n = 12	Standard deviation
Rock type	BA	A	BA		
*VU	Tcb	Tcb	Tcb		
Major elements (wt.%)					
SiO_2	55.20	59.90	56.41	57.59	2.42
TiO_2	1.35	1.22	1.38	1.27	0.09
Al_2O_3	16.25	15.85	16.96	16.03	0.53
Fe_2O_3	8.02	6.84	8.73	7.08	1.13
MnO	0.13	0.11	0.09	0.12	0.06
MgO	4.65	3.84	3.64	4.16	0.71
CaO	6.15	5.06	6.66	5.96	0.76
Na_2O	3.13	3.17	3.11	3.23	0.19
K_2O	2.13	2.04	2.25	1.91	0.28
P_2O_5	0.36	0.35	0.42	0.39	0.05
LOI	2.00	1.48	1.02		
Total	99.37	99.86	100.7		
CIPW normative minerals (calculated with the SINCLAS program)					
qz	9.358	17.274	10.617	14.473	4.66
or	12.989	12.304	13.415	11.572	1.68
ab	27.340	27.374	26.544	28.118	1.70

Table 3a (*continued*)

Sample	SLP0214	SLP0217	B35	Mean n = 12	Standard deviation
Rock type	BA	A	BA		
*VU	Tcb	Tcb	Tcb		
an	24.771	23.288	25.900	24.05	1.88
ne	–	–	–	–	–
di	3.430	-	3.755	2.95	2.00
hy	13.897	12.348	11.044	12.16	1.95
ol	–	–	–	–	–
Trace elements (ppm)					
Rb	63.00	73.00	72.00	69.00	18.00
Ba	720.00	1020.00	850.00	843.08	162.19
Th	7.25	10.35	10.00	7.80	2.10
Nb	15.00	15.30	15.00	14.10	1.70
La	35.00	43.00	40.57	41.01	8.10
Ce	73.00	94.00	53.60	83.05	20.65
Sr	416.00	427.00	456.00	625.00	271.00
Nd	39.00	47.00	21.29	42.52	10.65
Sm	7.40	8.40	4.90	8.00	1.54
Zr	285.00	326.00	259.00	277.00	52.00
Eu	1.75	1.73	1.23	1.85	0.29
Gd	6.65	6.60	4.36	6.38	0.78
Dy	5.20	5.00	3.83	4.74	0.45
Y	28.50	28.50	32.00	27.00	3.00
Er	2.80	2.60	1.96	0.30	0.30
Yb	2.42	2.34	1.55	0.31	0.31
Sc	20.00	16.00	2.00	5.33	5.33
V	150.00	123.00	5.00	131.00	52.00
Cr	170.00	116.00	4.00	63.00	63.00
Co	22.00	17.00	2.00	6.84	6.84
Ni	79.00	36.00	1.00	53.3	25.30
A.I.	2.280	1.720	2.290		
Mg#	65.393	65.350	57.897		
DI	49.687	56.952	50.576		

The geochemical analyses were performed at Université de Bretagne Occidental; analytic method described by Cotten et al. (1995). Chemical classification of rock types of total alkalis vs. silica diagram (Le Bas et al., 1986); BA, basaltic-andesite; A, andesite; TB, trachy-basalt; BSN, basanite; mnp, melanephelinite; alk, alkali; subal, subalkali. *Volcanic unit from the stratigraphy of the SLPVF (Labarthe-Hernández et al., 1982; Tristán-González et al., 2009a,b); Tcb, Casita Blanca andesite; Tbp, La Placa basalt; Tcb, Cabras basalt; Tle, Los Encinos basalt; Qbj, Las Joyas basalt; **VE, volcanic episode (see the text). SINCLAS program (Verma et al., 2002). A.I., Alkali Index of Middlemost (1975), A.I. = $(Na_2O + K_2O) / [(SiO_2 - 43) \times 0.17]$; Mg# = $100 \times (Mg^{2+}/Mg^{2+}+Fe^{2+})$; FeO = $Fe_2O_{3(total)} \times 0.85$. DI, diferentiation index, DI = $qz + or + ab + ne + lc$ (Thornton and Tuttle, 1960).

(2009a). In general, the andesites of Episode 1 are propilitized, green to gray, porphyritic rocks, containing up to 5 vol.% phenocrysts, 1–2 mm in size, of hornblende, biotite and plagioclase, microcrystal aggregates of plagioclase and biotite, and sometimes isolated pyroxene (titano-augite), within an aphanitic microcrystalline matrix (Fig. 3A). The Casita Blanca andesite crops out discontinuously in isolated windows and it overlies continental lacustrine sediments of the Cenicera Formation. It is best exposed in the Ahualulco volcanic complex (Tristán-González et al., 2009a). In some localities it is interbedded with reddish-brown continental conglomeratic deposits. The second age group is similar to the Casita Blanca andesite. It was emplaced around 36.4 ± 1.4 and the last event in this episode at 31.2 ± 0.7 Ma (Tables 1 and 2; Fig. 2). The neighboring Río Santa María Volcanic Field, at the opposite side of the Villa de Reyes graben (Fig. 1), includes two other andesitic units corresponding to this suite, 31.9 Ma Santa Catarina andesite and 31.6 Ma Mosco andesite, both associated with the Atotonilco volcano (Labarthe-Hernández et al., 1984, 1999). Near Villa Hidalgo to the north of San Luis Potosí City two other andesitic lavas dated at 31.6 and 30.5 Ma (Tristán-González et al., 2009a; Table 1), are also included in this episode.

5.2. Episode 2

It is represented by lavas of the La Placa basalt, which were extruded between 29.5 ± 0.7 and 28.0 ± 0.6 Ma. Although these lava rocks were first defined as basalts due to their mafic appearance (Tristán-González and Labarthe-Hernández, 1979), they are basaltic andesites and andesites (see geochemistry section below) and the name should be changed to the La Placa andesite. Episode 2 lavas are part of a bimodal succession that includes rhyolitic ignimbrite flows of about the same age (Tristán-González et al., 2009a). Episode 2 coincides with a peak in maximum extension in the region (Labarthe-Hernández et al., 1982; Tristán-González et al., 2009b). These lavas crop out mainly in the central portion of Sierra San Miguelito within the SLPVF (Labarthe-Hernández and Jiménez-López, 1992; Torres-Aguilera, 2005; Rodríguez-Ríos and Torres-Aguilera, 2009; Tristán-González et al., 2009a). The lavas are dark gray, with a trachytic texture and contain phenocrysts (1–2 mm) of plagioclase with reaction rims, and olivine altered to bitownite (Fig. 3B). It is best exposed in the Bledos graben and along the Juachín creek (Fig. 1).

5.3. Episode 3

It includes the lavas of the Cabras basalt, which were extruded around 22.1 ± 0.5 Ma and 21.6 ± 0.5 Ma (Table 2). These basalts were erupted from fissures following a peak of extension in the region (Labarthe-Hernández et al., 1982; Tristán-González et al., 2009b). Previous geochemical data indicate a slightly alkaline to alkaline composition, classifying it as trachybasalt to basaltic trachyandesite (Torres-Aguilera, 2005). It is black with holocrystalline, inequigranular, glomero-porphyritic and pilotaxitic textures, containing phenocrysts of plagioclase, mainly andesine, and olivine altered to boliwgnita (Fig. 3C). The olivine is subhedral. The groundmass is composed of microlitic olivine, plagioclase, titanomagnetite and interstitial clinopyroxene as egirina and augite.

5.4. Episode 4

It includes the Los Encinos lavas dated at around 12.0 Ma (Table 2). This suite also includes fissure-fed lava flows with a basaltic-andesitic

Table 3b
Major and trace element analyses of andesitic and basaltic volcanic rocks from the SLPVF. Episode 2, La Placa basalt.

Sample	SLP0305	GME0351	GME0352	GME0328	VB42	VB43	VB45	VB47	Mean n = 8	Standard deviation
Rock type	A	BA	BA	A	BA	BA	BA	A		
VU	Tbp	Tbp	Tbp	Tbp	Tbp	Tbp	Tbp	Tbp		
Major elements (wt.%)										
SiO_2	56.20	52.80	53.40	59.40	54.52	53.28	54.39	55.59	54.95	2.14
TiO_2	1.29	1.92	1.94	0.88	1.54	1.63	1.61	1.59	1.55	0.34
Al_2O_3	15.90	15.35	15.30	15.20	15.65	15.49	15.49	16.14	15.57	0.32
Fe_2O_3	8.07	9.65	9.96	7.12	8.65	9.45	9.34	9.48	8.97	0.96
MnO	0.12	0.14	0.15	0.11	0.13	0.13	0.12	0.14	0.13	0.01
MgO	3.12	4.58	5.32	3.52	6.52	3.97	5.79	2.63	4.43	1.36
CaO	6.27	8.39	7.40	6.65	7.29	9.17	7.69	7.36	7.53	0.92
Na_2O	2.52	2.67	2.70	2.14	2.30	2.64	2.66	2.77	2.55	0.22
K_2O	2.20	1.42	1.27	2.98	1.30	1.44	1.57	1.71	1.74	0.58
P_2O_5	0.34	0.52	0.50	0.23	0.41	0.43	0.43	0.42	0.41	0.09
LOI	3.58	1.97	1.68	1.53	1.92	2.49	1.20	1.94		
Total	99.61	99.41	99.62	99.76	100.00	100.00	100.00	99.82		
CIPW normative minerals (calculated with the SINCLAS program)										
qz	15.709	9.454	10.221	17.376	11.261	9.685	9.151	14.328	12.14	3.19
or	13.610	8.669	7.712	18.007	7.866	8.805	9.432	10.424	10.56	3.54
ab	22.322	23.337	23.481	18.514	19.953	23.050	22.880	24.107	22.20	1.94
an	26.771	26.546	26.596	23.584	29.166	26.914	26.039	27.285	26.61	1.53
ne	–	–	–	–	–	–	–	–	–	–
di	2.801	10.409	6.240	6.922	4.088	13.795	7.854	6.022	7.26	3.49
hy	10.690	11.413	15.473	9.053	19.168	8.449	15.454	8.337	12.25	3.99
ol	–	–	–	–	–	–	–	–	–	–
Trace elements (ppm)										
Rb	125.00	40.50	37.50	117.00	106.00	45.00	71.00	57.00	75.00	36.00
Ba	680.00	742.00	510.00	585.00	487.00	1297.00	502.00	423.00	653.25	280.70
Th	7.10	4.00	3.85	9.70	5.00	7.00	1.50	7.00	5.60	2.60
Nb	13.00	17.00	17.00	11.70	15.00	13.00	13.00	16.00	14.5	2.10
La	28.00	32.00	31.00	29.00	40.22	33.29	52.69	42.49	36.09	8.45
Ce	61.00	69.00	66.00	58.00	78.35	64.45	89.23	71.27	69.66	10.09
Sr	442.00	564.00	548.00	345.00	469.00	440.00	416.00	423.00	456.00	71.00
Nd	34.00	41.50	41.50	30.00	39.69	34.85	46.84	41.41	38.72	5.38
Sm	6.70	8.60	8.60	6.50	8.65	7.81	9.67	8.51	8.13	1.07
Zr	220.00	282.00	270.00	188.00	270.00	212.00	222.00	237.00	238.00	33.00
Eu	1.69	2.24	2.25	1.43	2.10	2.01	1.96	2.06	1.97	0.28
Gd	6.40	8.30	8.10	6.30	5.57	6.68	6.34	6.88	6.83	0.93
Dy	5.10	6.75	6.90	5.50	4.46	6.24	5.27	6.15	5.80	0.85
Y	28.50	39.00	39.00	33.50	53.00	38.00	34.00	39.00	38.00	7.00
Er	2.70	3.60	3.70	3.00	2.05	2.99	2.46	2.98	2.94	0.55
Yb	2.46	3.33	3.40	2.80	2.14	2.90	2.51	2.85	2.80	0.43
Sc	22.00	24.00	24.00	20.00	–	–	–	–	22.50	1.91
V	126.00	173.00	188.00	135.00	156.00	160.00	171.00	139.00	156.00	21.00
Cr	206.00	152.00	181.00	90.00	223.00	267.00	258.00	246.00	203.00	60.00
Co	23.00	25.00	27.00	17.00	35.00	28.00	34.00	39.00	28.5	7.17
Ni	27.50	34.00	44.00	7.00	53.00	86.00	87.00	96.00	54.3	32.30
A.I.	1.830	2.150	1.690	1.740	1.390	1.810	1.720	1.770		
Mg#	55.447	59.391	62.206	62.265	69.799	56.533	65.994	46.906		
DI	51.641	41.460	41.414	53.897	39.080	41.540	41.463	48.859		

The geochemical analyses were performed at Université de Bretagne Occidental; analytic method described by Cotten et al. (1995). Chemical classification of rock types of total alkalis vs. silica diagram (Le Bass et al., 1986); BA, basaltic-andesite; A, andesite; TB, trachy-basalt; BSN, basanite; mnp, melanephelinite; alk, alkali; subal, subalkali. Volcanic unit from the stratigraphy of the SLPVF (Labarthe-Hernández et al., 1982; Tristán-González et al., 2009a,b); Tcb, Casita Blanca andesite; Tbp, La Placa basalt; Tcb, Cabras basalt; Tle, Los Encinos basalt; Qbj, Las Joyas basalt (see the text). SINCLAS program (Verma et al., 2002). A.I., Alkali Index of Middlemost (1975), A.I. = $(Na_2O + K_2O)$ / $[(SiO_2 - 43) \times 0.17]$; Mg# = $100 \times (Mg^{2+} / Mg^{2+}+Fe^{2+})$; FeO = $Fe_2O_{3(total)} \times 0.85$. DI, diferentiation index, DI = $qz + or + ab + ne + lc$ (Thornton and Tuttle, 1960).

composition extruded along NNW trending faults and/or fissures, which formed scoria cones and blocky lava flows (Aguillón-Robles et al., 2012). The alkaline rocks have been related to an intra-plate magmatic event during the middle Miocene and subsequent to volcanism of the SLPVF (Luhr et al., 1995). The lavas both basalt and basaltic andesites, are porphyritic containing ca. 20 vol.% of phenocrysts of plagioclase, olivine, hornblende and augite, in a fine, plagioclase-augite-bearing microlitic groundmass (Fig. 3D; Sánchez-García, 2009).

5.5. Episode 5

This episode starts with basaltic lavas of 5.05 Ma age (Table 2) and volcanism continued until the Pleistocene with pyroclastic rocks and lavas of Las Joyas basalt (Labarthe-Hernández et al., 1982). Although the Las Joyas basalt was previously interpreted as a single episode around 1.5 Ma (Table 1; Tristán-González et al., 2009a), the new ages presented reveal younger ages, ranging between 1.01 ± 0.10 and 0.6 ± 0.06 Ma (Table 2). Episode 5 includes lavas and pyroclastic material extruded from monogenetic vents, such as maars and tuff cones, but also through dikes. The vents are associated with NNW regional faults. This basaltic volcanism occurred mainly in the northern portion of the SLPVF. Phreatomagmatic products of the Las Joyas basalt contain xenoliths from the mantle and/or the lower crust, particularly at the La Joya maar (Aranda-Gómez et al., 2005; Saucedo-Girón et al., 2011). The lavas are black and vesicular, generally with holocrystalline or inequigranular textures, such as microporphyritic

Table 3c
Major and trace element analyses of andesitic and basaltic volcanic rocks from the SLPVF. Episode 3, Cabras basalt.

Sample	SLP0303	VB21Tbc	VB23	VB31	VB35	SLP06-01	Mean n = 6	Standard deviation
Rock type	BTA, sho	TB, pot	TB, pot	TB, pot	TB, pot	BTA, sho		
VU	Tbc	Tbc	Tbc	Tbc	Tbc	Tbc		
Major elements (wt.%)								
SiO_2	52.80	45.87	47.51	47.85	45.87	49.15	48.18	2.59
TiO_2	2.52	2.37	3.27	3.18	2.37	2.84	2.76	0.40
Al_2O_3	13.35	14.54	14.68	14.80	15.54	16.05	14.83	0.93
Fe_2O_3	14.88	12.58	15.91	15.86	12.58	13.6	14.24	1.53
MnO	0.20	0.18	0.21	0.20	0.18	0.19	0.20	0.01
MgO	2.16	6.31	3.76	3.60	6.31	2.12	4.05	1.89
CaO	6.05	7.99	6.95	6.72	7.99	6.70	7.07	0.78
Na_2O	2.24	3.66	3.80	3.78	3.66	4.00	3.52	0.64
K_2O	3.03	1.81	2.04	2.11	1.81	2.71	2.25	0.50
P_2O_5	1.35	1.01	1.56	1.59	1.01	1.02	1.26	0.28
LOI	0.70	3.25	1.19	−0.15	3.25	1.34		
Total	99.28	100.00	99.39	99.57	100.62	99.72		
CIPW normative minerals (calculated with the SINCLAS program)								
qz	13.888	–	0.076	0.761	–	0.634	3.83	6.70
or	18.338	11.193	12.239	12.646	11.075	16.417	13.65	3.00
ab	19.411	29.952	32.586	32.408	28.979	34.692	29.67	5.42
an	17.838	18.727	17.179	17.391	21.356	18.279	18.46	1.52
ne	–	1.344	–	–	1.692	–	1.51	0.24
di	3.224	12.758	6.044	4.793	10.354	7.384	7.42	3.56
hy	10.750	–	13.186	13.378	–	6.588	10.97	3.16
ol	–	12.005	–	–	12.665	–	12.33	0.46
Trace elements (ppm)								
Rb	73.00	55.00	25.00	26.00	74.00	41.50	49.00	22.00
Ba	1030.00	1207.00	802.00	754.00	595.00	965.00	595.00	218.61
Th	5.00	2.00	3.00	1.00	6.00	4.50	3.60	1.90
Nb	54.00	53.00	38.00	38.00	77.00	40.00	50.00	15.10
La	66.00	61.66	27.71	71.00	53.63	52.00	53.33	15.34
Ce	138.00	130.32	50.93	136.84	102.57	107.00	110.94	33.06
Sr	365.00	415.00	533.00	525.00	1220.00	470.00	588.00	316.00
Nd	80.00	68.31	32.76	81.76	46.09	66.00	62.49	19.38
Sm	17.00	15.19	7.14	17.31	9.06	14.20	13.32	4.24
Zr	620.00	478.00	335.00	331.00	315.00	465.00	424.00	120.00
Eu	4.00	4.04	2.12	4.90	3.20	3.64	3.65	0.94
Gd	16.00	13.74	6.05	14.89	7.47	13.60	11.96	4.14
Dy	13.60	12.80	5.20	12.54	5.67	11.30	10.19	3.76
Y	76.00	71.00	68.00	62.00	36.00	67.00	63.00	14.00
Er	7.00	6.18	2.41	5.40	2.38	6.2	4.93	2.03
Yb	6.24	5.76	2.04	4.74	2.14	5.50	4.40	1.86
Sc	24.00	–	–	–	–	22.50	23.25	1.06
V	60.00	66.00	155.00	137.00	144.00	94.00	109.00	41.00
Cr	4.00	7.00	15.00	13.00	134.00	26.00	33.00	50.00
Co	19.00	22.00	27.00	24.00	30.00	30.00	26.83	7.08
Ni	3.00	5.00	10.00	11.00	67.00	22.00	19.70	24.10
A.I.	2.870	4.290	5.150	4.990	4.550	4.860		
Mg#	31.775	60.778	42.757	41.858	60.776	33.923		
DI	51.637	42.489	44.901	45.815	41.746	51.743		

The geochemical analyses were performed at Université de Bretagne Occidental; analytic method described by Cotten et al. (1995). Chemical classification of rock types of total alkalis vs. silica diagram (Le Bass et al., 1986); BA, basaltic-andesite; A, andesite; TB, trachy-basalt; BSN, basanite; mnp, melanephelinite; alk, alkali; subal, subalkali. VU, volcanic unit from the stratigraphy of the SLPVF (Labarthe-Hernández et al., 1982; Tristán-González et al., 2009a,b); Tcb, Casita Blanca andesite; Tbp, La Placa basalt; Tcb, Cabras basalt; Tle, Los Encinos basalt; Qbj, Las Joyas basalt (see the text). SINCLAS program (Verma et al., 2002). A.I., Alkali Index of Middlemost (1975), A.I. = $(Na_2O + K_2O) / [(SiO_2 - 43) \times 0.17]$; Mg# = $100 \times (Mg^{2+} / Mg^{2+}+Fe^{2+})$; FeO = $Fe_2O_{3(total)} \times 0.85$. DI, diferentiation index, DI = $qz + or + ab + ne + lc$ (Thornton and Tuttle, 1960).

and pilotaxitic. Olivine is the only phenocrystic phase and is altered to iddingsite. The groundmass is composed of microlites of calcic plagioclase, with pigeonite or augite filling the interstices between plagioclase (Fig. 3E). The Las Joyas basalt, both the 5.05 Ma and the Pleistocene lavas, are silica undersaturated, with compositions of hawaiite, alkaline basalt and basalt.

6. Major and trace element geochemistry

Whole rock chemical analyses were done on representative samples collected from the andesitic and basaltic units of the SLPVF (Tables 3a, 3b, 3c, 3d, 3e). Using the TAS classification of Le Bass et al. (1986) the samples with $SiO_2 < 53$ wt.% include basalt, trachybasalt, hawaiite, and basanite; those with $SiO_2 = 53–57$ wt.%, include basaltic andesite and trachybasaltic andesite; and those with $SiO_2 = 57–63$ wt.%, include andesite and trachyandesite (Fig. 4).

Bi-element variation diagrams (Harker, 1909; Fig. 4) show particular trends in the major elements for each of the five volcanic episodes, suggesting syn-tectonic magmatic events. The SiO_2-K_2O variation diagram and superimposed classification of Peccerillo and Taylor (1976) indicate that the five episodes have contents of K_2O ranging from low to high (Fig. 4). The Alumina Index vs. Al_2O_3 diagram and basalt classification of Middlemost (1975) indicates that many samples are high-alumina basalts, but the data spread across and into the flood-basalt composition

Table 3d
Major and trace element analyses of andesitic and basaltic volcanic rocks from the SLPVF. Episode 4, Los Encinos basalt.

Sample	GME0341	GME0342	GME0343	RV08	RV09	RV10	Mean $n = 6$	Standard deviation
Rock type	A	BA	A	B	A	B		
VU	Tle	Tle	Tle	Tle	Tle	Tle		
Major elements (wt.%)								
SiO_2	57.80	56.20	60.70	49.40	57.69	47.60	54.59	5.20
TiO_2	1.29	1.42	1.32	1.94	1.48	2.04	1.58	0.33
Al_2O_3	17.00	17.35	16.55	15.60	15.85	13.98	16.06	1.21
Fe_2O_3	7.00	8.40	6.40	11.85	7.04	12.10	8.80	2.55
MnO	0.10	0.12	0.09	0.17	0.09	0.19	0.13	0.04
MgO	3.45	4.35	2.57	6.29	3.08	8.60	4.72	2.31
CaO	6.30	6.60	4.95	9.40	7.11	8.90	7.21	1.67
Na_2O	3.45	2.83	3.22	3.45	3.56	3.30	3.30	0.26
K_2O	2.50	1.64	2.74	1.18	2.00	1.57	1.94	0.59
P_2O_5	0.31	0.31	0.34	0.41	0.42	0.58	0.40	0.10
LOI	0.80	0.80	0.87	−0.09	1.83	0.03		
Total	100.00	100.02	99.75	99.60	100.17	98.89		
CIPW normative minerals (calculated with the SINCLAS program)								
qz	10.682	12.312	17.475	–	10.985	–	12.863	3.15
or	14.952	9.822	16.435	7.068	12.085	9.485	11.641	3.54
ab	29.548	24.259	27.653	29.582	30.809	24.229	27.680	2.84
an	23.806	30.187	22.676	23.908	21.844	19.110	23.588	3.67
ne	–	–	–	–	–	2.336	2.336	–
di	4.613	0.751	–	16.932	9.327	36.012	13.527	13.94
hy	8.899	14.528	8.264	2.114	8.579	–	8.476	4.39
ol	–	–	–	13.045	–	18.764	15.904	4.04
Trace elements (ppm)								
Rb	71.00	45.00	73.00	19.25	46.71	30.12	48.00	21.00
Ba	700.00	830.00	950.00	603.78	1313.17	901.47	883.07	246.63
Th	5.60	5.00	7.90	2.6	5.29	3.43	5.00	1.80
Nb	11.50	11.00	14.00	16.29	9.97	30.32	15.50	7.60
La	28.00	26.00	37.50	21.98	36.74	33.04	30.54	6.22
Ce	54.00	55.00	76.50	42.10	75.47	59.59	60.44	13.36
Sr	540.00	488.00	480.00	610.49	747.95	862.84	622.00	154.00
Nd	29.50	30.00	40.00	22.37	40.11	31.71	32.28	6.82
Sm	6.00	5.90	7.40	5.34	7.71	6.57	6.49	0.92
Zr	185.00	205.00	270.00	165.38	311.17	198.64	223.00	56.00
Eu	1.71	1.77	1.87	1.61	1.88	1.88	1.79	0.11
Gd	5.30	5.70	6.30	5.23	5.98	5.81	5.72	0.41
Dy	3.95	4.40	4.20	4.14	3.66	3.95	4.05	0.26
Y	22.00	25.00	22.00	22.80	13.64	15.95	20.00	4.00
Er	1.90	2.20	1.80	2.17	1.77	1.99	1.97	0.18
Yb	1.75	2.05	1.58	2.02	1.64	1.76	1.80	0.19
Sc	15.50	18.50	11.80	–	–	–	15.27	3.36
V	146.00	165.00	95.00	165.42	79.58	167.85	136.00	39.00
Cr	60.00	108.00	38.00	450.28	174.90	468.89	217.00	194.00
Co	17.00	20.00	13.00	45.85	20.15	59.58	29.27	18.86
Ni	25.00	26.00	12.00	31.35	16.40	89.05	33.30	28.2
A.I.	2.280	1.910	1.910	2.96	2.01	3.62		
Mg#	62.643	62.299	58.26	61.974	59.429	68.503		
DI	55.182	46.393	61.563	2.98	2.04	3.65		

The geochemical analyses were performed at Université de Bretagne Occidental; analytic method described by Cotten et al. (1995). The samples RV08 and RV10, were reported in Aguillón-Robles et al. (2012). Chemical classification of rock types of total alkalis vs. silica diagram (Le Bass et al., 1986); BA, basaltic-andesite; A, andesite; TB, trachy-basalt; BSN, basanite; mnp, melanephelinite; alk, alkali; subal, subalkali. VU, Volcanic Unit from the stratigraphy of the SLPVF (Labarthe-Hernández et al., 1982; Tristán-González et al., 2009a,b); Tcb, Casita Blanca andesite; Tbp, La Placa basalt; Tcb, Cabras basalt; Tle, Los Encinos basalt; Qbj, Las Joyas basalt (see the text). SINCLAS program (Verma et al., 2002). A.I., Alkali Index of Middlemost (1975), A.I. = $(Na_2O + K_2O) / [(SiO_2 - 43) \times 0.17]$; Mg# = $100 \times (Mg^{2+} / Mg^{2+} + Fe^{2+})$; FeO = $Fe_2O_{3(total)} \times 0.85$. DI, diferentiation index, DI = $qz + or + ab + ne + lc$ (Thornton and Tuttle, 1960).

(Fig. 5), with a variation in the Alumina Index of 1.7 to 8, where the basanitic lavas yielded the highest values (Tables 3a, 3b, 3c, 3d, 3e).

6.1. Chemical characteristics Episode 1

It shows major element features of the calc-alkaline series with low Na_2O/K_2O ratio, and low to moderate K_2O content. Harker diagrams display TiO_2, Fe_2O_3*, MgO, MnO, and CaO the typical negative correlations with SiO_2, while K_2O and to a lesser extent Na_2O the positive ones (Fig. 4). The CIPW norm minerals calculated for Episode 1 are silica-saturated, calc-alkaline, in terms of the Peacock index (Yoder and Tilley, 1962; Barker, 1983). Although it was informally named as the Casita Blanca andesite due to its field appearance (Labarthe-Hernández et al., 1982), its chemical composition indicates that these lavas range from basaltic-andesite to dacite (Fig. 4; Table 3a). The oldest lavas of this episode have characteristics of flood-basalts in the Alumina Index vs. Al_2O_3 plot (Middlemost, 1975; Fig. 5). The lava flows of Late Eocene are slightly more enriched in SiO_2 with time from ca. 43 to 31 Ma

Table 3e
Major and trace analyses of andesitic and basaltic volcanic rocks from the SLPVF. Episode 5, Las Joyas basalt.

Sample	GME0344	GME0348	GME0349	SLP0210	B23	Mean $n = 5$	Standard deviation
Rock type	BSN, bsn	BSN, mnp	BSN, bsn	TB, haw	TB, pot		
VU	Qbj	Qbj	Qbj	Qbj	Qbj		
Major elements (wt.%)							
SiO_2	44.80	41.90	44.50	45.90	45.99	44.62	1.66
TiO_2	2.30	2.96	3.03	2.42	2.37	2.62	0.35
Al_2O_3	14.00	11.85	14.12	13.40	13.33	13.34	0.90
Fe_2O_3	13.40	13.50	12.92	11.85	12.71	12.88	0.66
MnO	0.21	0.20	0.20	0.18	0.18	0.19	0.01
MgO	7.78	12.90	8.47	9.60	9.67	9.68	1.97
CaO	9.80	8.70	9.20	9.05	8.78	9.11	0.44
Na_2O	4.35	4.46	4.32	3.85	3.26	4.05	0.50
K_2O	1.95	2.30	2.19	1.43	1.70	1.91	0.36
P_2O_5	0.91	1.15	1.03	1.18	1.22	1.10	0.13
LOI	0.67	−0.38	−0.11	0.79	0.19		
Total	100.17	99.54	99.87	99.65	99.42		
CIPW normative minerals (calculated with the SINCLAS program)							
qz	–	–	–	–	–	–	–
or	11.678	13.722	13.048	8.616	10.212	11.455	2.08
ab	14.228	3.206	14.050	24.201	24.728	16.082	8.86
an	13.094	5.573	12.775	15.348	16.993	12.756	4.36
ne	12.503	18.900	12.356	4.882	1.795	10.087	6.79
di	24.162	24.062	21.032	17.945	15.301	20.500	3.87
hy	–	–	–	–	–	–	–
ol	10.451	18.867	11.445	15.328	17.007	14.619	3.59
Trace elements (ppm)							
Rb	34.50	36.50	49.50	27.50	148.00	59.00	50.00
Ba	1200.00	485.00	573.00	480.00	607.00	669.00	301.91
Th	7.60	7.40	6.70	7.05	8.00	7.40	0.50
Nb	82.00	95.00	84.00	70.00	73.00	80.8	9.90
La	60.00	60.00	56.00	54.00	32.91	52.58	11.30
Ce	105.00	114.00	110.00	105.00	67.92	100.38	18.54
Sr	995.00	976.00	970.00	940.00	949.00	966.00	22.00
Nd	50.50	57.50	56.00	49.50	26.69	48.04	12.42
Sm	9.30	11.00	10.75	9.70	6.12	9.37	1.95
Zr	265.00	335.00	345.00	310.00	264.00	304.00	38.00
Eu	2.94	3.38	3.35	2.95	1.97	2.92	0.57
Gd	8.10	9.10	9.35	8.20	5.56	8.06	1.50
Dy	6.10	6.20	6.70	6.10	4.51	5.92	0.83
Y	32.50	30.00	33.00	31.50	35.00	32.00	2.00
Er	2.80	2.70	3.00	2.80	2.02	2.66	0.38
Yb	2.36	1.95	2.30	2.23	1.42	2.05	0.39
Sc	19.50	16.50	20.00	20.00	2.00	15.60	7.74
V	202.00	197.00	220.00	192.00	5.00	163.00	89.00
Cr	216.00	480.00	191.00	370.00	4.00	2.52.00	182.00
Co	44.00	57.00	46.50	45.00	2.00	38.90	21.27
Ni	156.00	424.00	147.00	240.00	1.00	193.60	154.90
A.I.	15.550		20.600	8.340	7.900		
Mg#	64.675	75.021	67.513	71.314	69.802		
DI	38.409	35.828	39.454	37.699	36.735		

The geochemical analyses were performed at Université de Bretagne Occidental; analytic method described by Cotten et al. (1995). Chemical classification of rock types of total alkalis vs. silica diagram (Le Bass et al., 1986); BA, basaltic-andesite; A, andesite; TB, trachy-basalt; BSN, basanite; mnp, melanephelinite; alk, alkali; subal, subalkali. VU, volcanic unit from the stratigraphy of the SLPVF (Labarthe-Hernández et al., 1982; Tristán-González et al., 2009a,b); Tcb, Casita Blanca andesite; Tbp, La Placa basalt; Tcb, Cabras basalt; Tle, Los Encinos basalt; Qbj, Las Joyas basalt (see the text). SINCLAS program (Verma et al., 2002). A.I., Alkali Index of Middlemost (1975), A.I. = $(Na_2O + K_2O) / [(SiO_2 - 43) \times 0.17]$; Mg# = $100 \times (Mg^{2+} / Mg^{2+} + Fe^{2+})$; FeO = $Fe_2O_{3(total)} \times 0.85$. DI, diferentiation index, DI = $qz + or + ab + ne + lc$ (Thornton and Tuttle, 1960).

(Fig. 4). Pearce elements ratio plots (Pearce, 1968; Pearce and Cann, 1973) suggest high fractionation of plagioclase, olivine, clinopyroxene and Fe–Ti oxides; and a low fractionation of apatite (Fig. 6).

Trace element analyses show that volcanic rocks of Episode 1 are enriched in compatible elements Cr and Ni, low contents of Co, variable contents of Rb, Ba, Th, Sr, La, and low contents of Zr and Nb (Fig. 7). In multi-element plots normalized to primitive mantle (Fig. 8; Sun and McDonough, 1989) the lavas of this group show highly fractionated patterns, with positive anomalies of most LILE (especially Rb and K), and negative anomalies in Nb, Ti (HFSE). On the other hand, the LREE are relatively more enriched than the HREE, which have slightly negative slope (Fig. 8).

6.2. Chemical characteristics of Episode 2

Major elements of Episode 2 show features of the sub-alkaline series; with low Na_2O/K_2O ratio, and low K_2O content. In the Harker diagrams it displays TiO_2, Fe_2O_3* MgO, CaO and P_2O_5 in less negative correlations with respect to SiO_2, while K_2O and Na_2O show less positive correlations (Fig. 4). The CIPW minerals of Episode 2 are silica-saturated in terms of the Peacock index (Yoder and Tilley, 1962; Barker, 1983). This episode was informally named La Placa basalt (Labarthe-Hernández et al., 1982) but the rocks are classified as andesite to basaltic-andesite with subalkaline characteristics (Fig. 4; Table 3b). Based on the Alumina Index trends, this episode has a flood-basalt affinity (Fig. 5). A negative

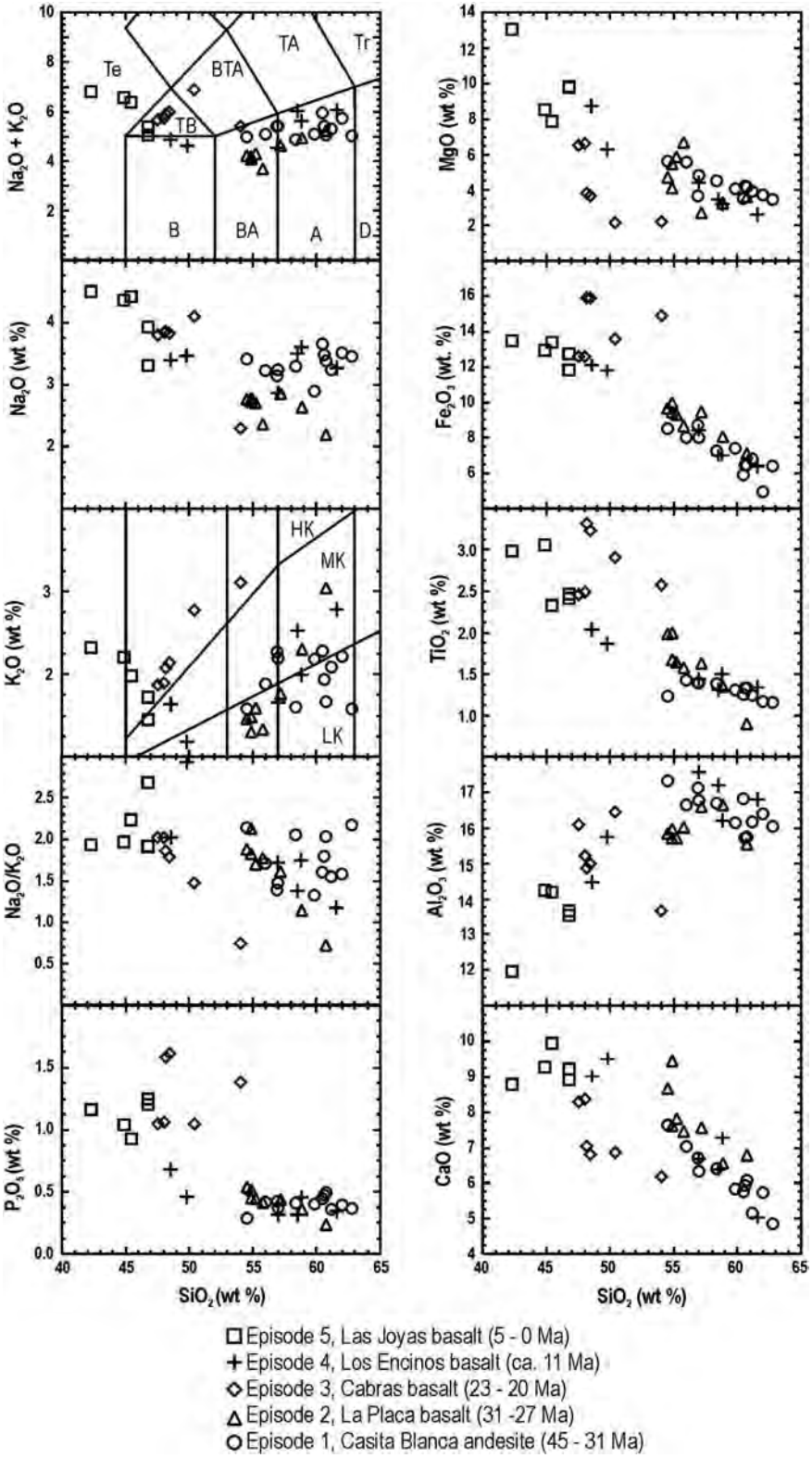

Fig. 4. Harker variation diagrams (Harker, 1909) with selected major elements for the five volcanic episodes of the SLPF, including the TAS classification diagram (Le Bass et al., 1986); Tr—trachyte, D—dacite, TA—trachyandesite, A—andesite, BTA—basalt-trachyandesite, BA—basalt-andesitic, B—basalt, TB—trachy-basalt, Te—tephrite. Also included is the K_2O vs. SiO_2 diagram with the classification of Peccerillo and Taylor (1976); LK—low potassium content, MK—moderate potassium content, HK—high potassium content.

tendency is observed in the incompatible elements with higher SiO_2 whereas the compatible ones increase. This suite shows crystal fractionation mainly of olivine, plagioclase, clinopyroxene and Fe–Ti oxides in the Pearce elements ratios plot (Fig. 6).

Trace elements show enrichment of compatible elements Cr, Co, Ni and depletion of Ba, Sr, and La with the increase of Mg# (Fig. 7). Multi-element patterns (normalized to Primitive Mantle) show light positive anomalies of LILE (Rb and K), which are almost flat, and

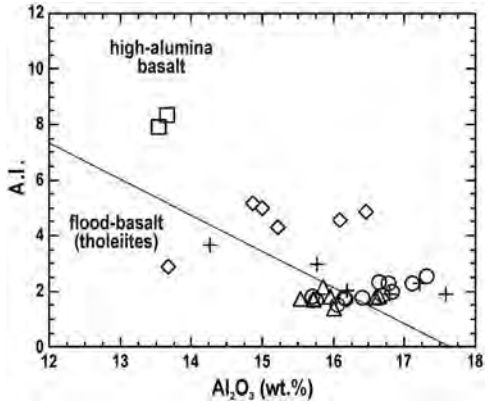

Fig. 5. Alumina vs. Alkali Index diagram and classification of basalts (Middlemost, 1975) for selected samples representing the five volcanic episodes of the SLPVF. Alkali Index is defined in Tables 3a, 3b, 3c, 3d, 3e.

negative anomalies of Nb, Sr and Ti. The REE patterns show a LREE more fractionated than the HREE with affinity to a volcanic arc (Fig. 8).

6.3. Chemical characteristics Episode 3

This group is alkaline, with low to high Na_2O/K_2O ratios and high MgO, $Fe_2O_3^*$, TiO_2, Na_2O and K_2O contents. According to the TAS classification the composition of Episode 3 volcanic rocks ranges from a K-rich trachybasalt to shoshonitic basaltic-trachyandesite (Table 3c; Fig. 4). The CIPW normative mineralogy resulted in a silica-undersaturated alkaline composition (Yoder and Tilley, 1962; Tables 3a, 3b, 3c, 3d, 3e). It shows a positive tendency in the incompatible elements with SiO_2 and a negative tendency in the compatible elements (Fig. 4). In the Alumina Index vs. Al_2O_3 diagram of Middlemost (1975) the volcanic rocks plot in the high-alumina basalt field (Fig. 5). Pearce elements ratio diagrams (Pearce, 1968; Pearce and Cann, 1973) indicate fractionation of plagioclase, olivine, clinopyroxene and Fe–Ti oxides (Fig. 6).

Episode 3 rocks have low contents of compatible trace elements Cr, Co and Ni, and relatively high contents of Zr and Nb. Mg# ranges from 30 to over 70 (Fig. 7). The multi-elemental plot normalized to Primitive

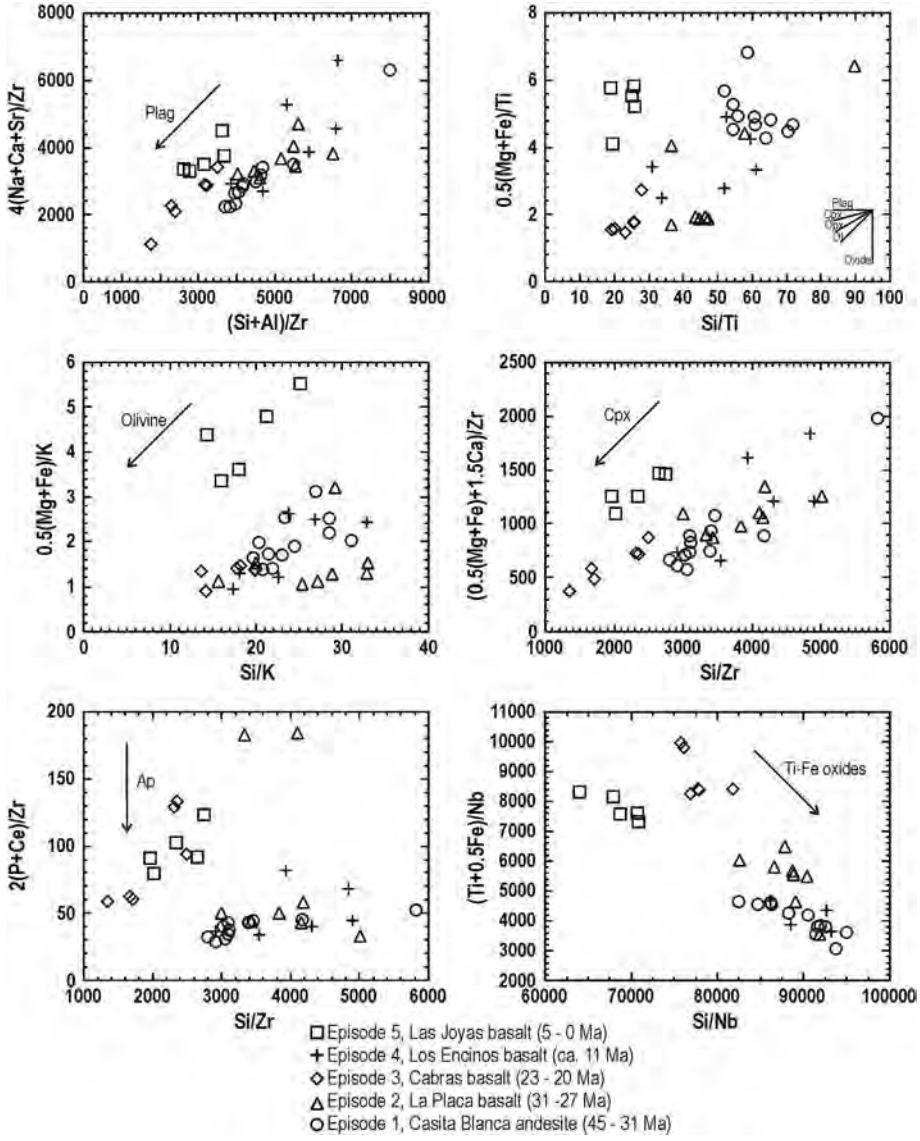

Fig. 6. Pearce Element Ratio diagram (Pearce, 1968; Pearce and Cann, 1973) showing crystal fractionation trends for plagioclase, olivine, clinopyroxene, apatite and Ti–Fe oxides for data from selected samples of the five volcanic episodes of the SLPVF.

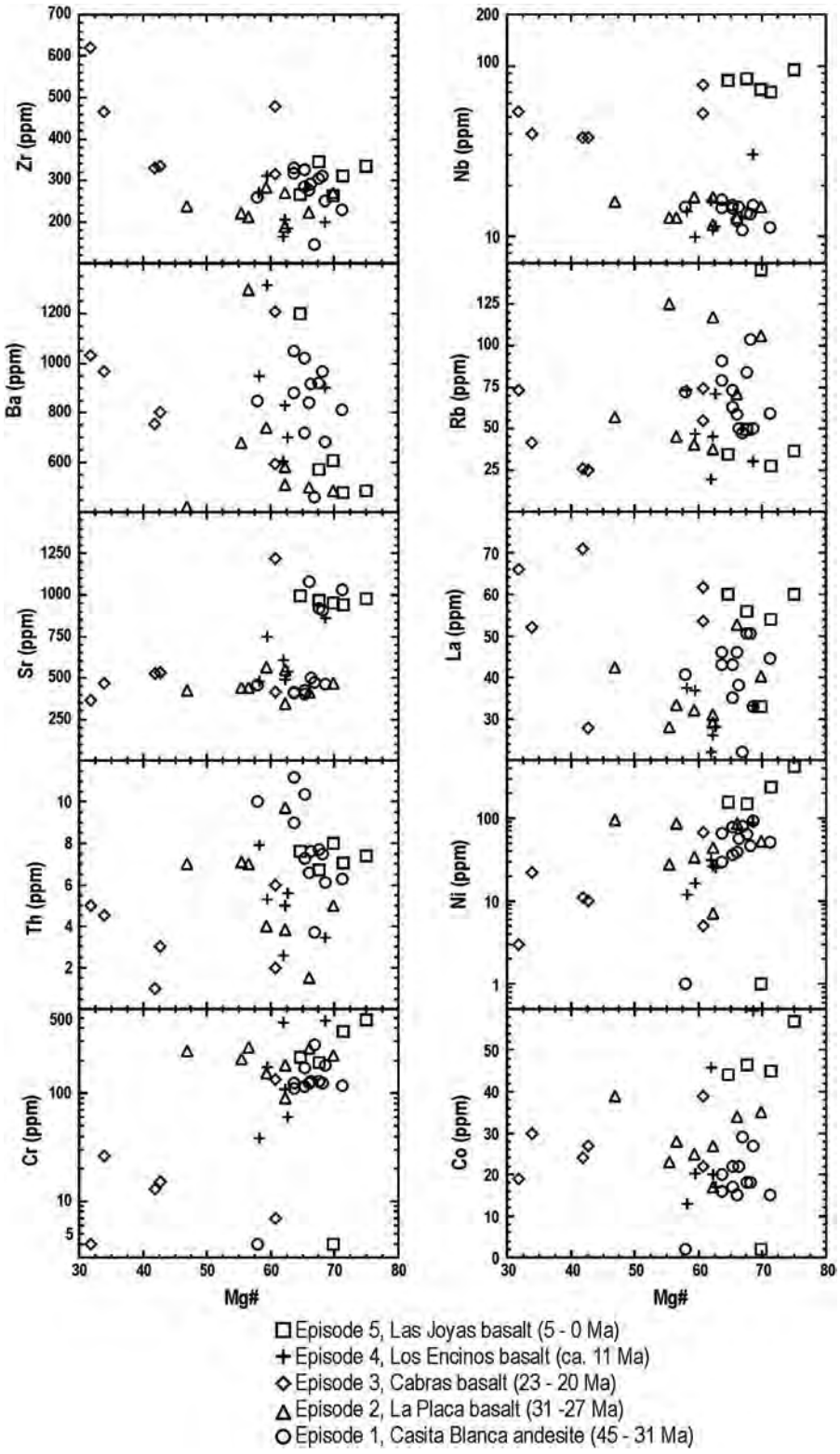

Fig. 7. Variation diagrams of Mg# vs. selected trace elements from representative samples of the five volcanic episodes of the SLPVF, where Mg# = [Mg / (Mg + Fe^{2+})] × 100 with Fe^{2+} = $Fe_2O_3^*$ × 0.85 (Wilkinson, 1982).

Mantle displays an almost flat pattern of incompatible elements and negative anomalies of Th and Sr (Fig. 8). The patterns of these lavas are enriched in the most incompatible elements as Ba, Nb, and LREE. This signature is commonly observed in intra-plate alkali basalts (e.g., Wilson, 1989; Gill, 2010; Winters, 2010).

6.4. Chemical characteristics of Episode 4

The sequence includes silica-saturated subalkaline basalts and silica-undersaturated (*ne*-normative) alkaline basalts. It shows high contents of incompatible major element oxides (TiO_2, Na_2O, K_2O; P_2O_5). FeO*/

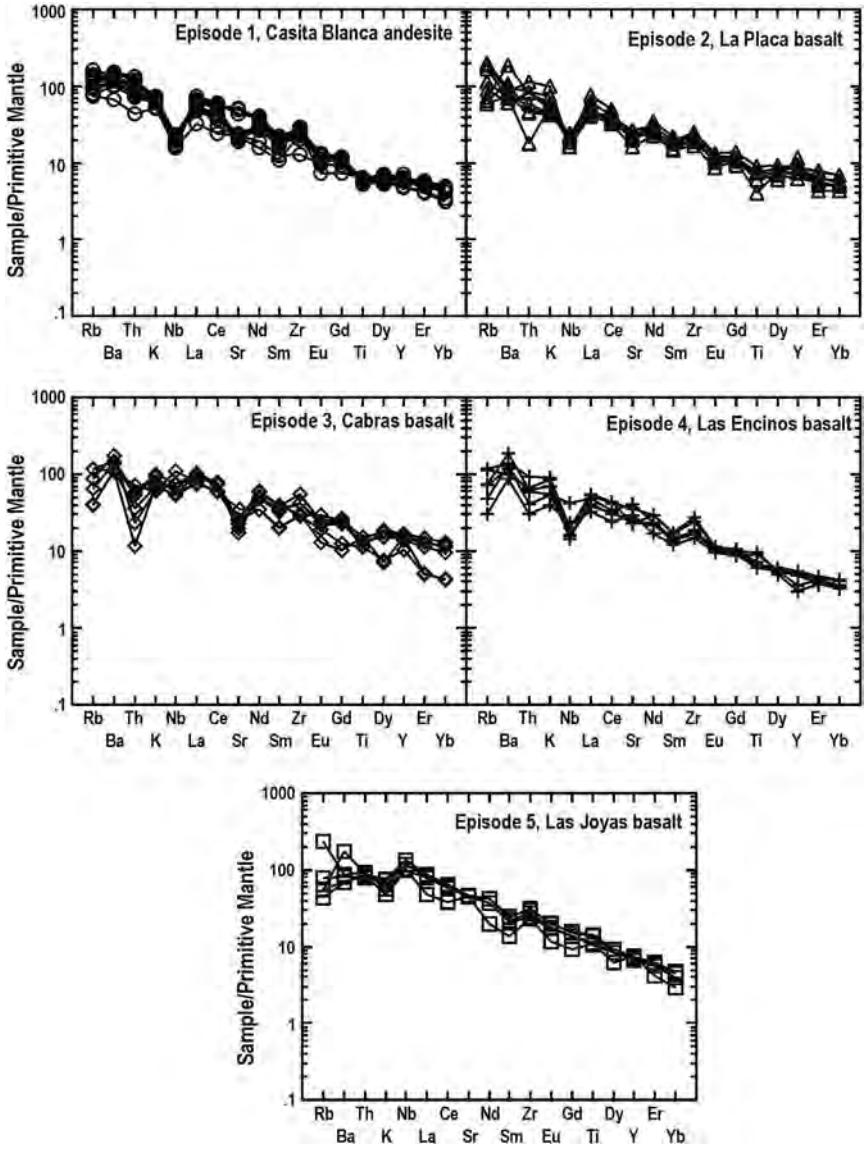

Fig. 8. Multi-element diagrams for representative samples of the five volcanic episodes of the SLPVF, normalized to Primitive Mantle using values of Sun and McDonough (1989).

MgO ratios are rather low (less than 1.3) and the Mg# varies by less than 10% from 68.5 to 59.4. In Harker diagrams (Fig. 4), TiO_2, $Fe_2O_3^*$, MgO, P_2O_5 and K_2O show negative correlations with SiO_2, and CaO and Al_2O_3 show positive ones; those features are consistent with differentiation- or assimilation-related processes. The chemical composition ranges from alkaline basalt to subalkaline basaltic andesite (Table 3d). The group falls under the high-alumina basalt field of the Alumina Index vs. Al_2O_3 plot (Fig. 5). Variation on Pearce element ratio diagrams are consistent with fractionation of olivine, clinopyroxene; plagioclase and Fe–Ti oxides (Fig. 6).

The rocks of this episode show enrichment of compatible trace elements Cr, Co, Ni, and a slight negative correlation of Sr, Th, Zr and Rb with Mg# (Fig. 7). In the Primitive Mantle normalized multi-element diagram (Fig. 8) Ba and Zr have slight positive anomalies and Nb a pronounced negative anomaly relative to K and La, and relatively more fractionation of the incompatible elements with respect to the compatible elements. The LREE are enriched whereas the HREE show a pronounced negative slope by depletion (Fig. 8). These characteristics are typical of alkaline suites (e.g., Wilson, 1989; Gill, 2010).

6.5. Chemical characteristics of Episode 5

Episode 5 displays high contents in incompatible major element oxides (TiO_2, Na_2O, K_2O, P_2O_5) and shows relatively high Na_2O/K_2O ratios (Table 3e; Fig. 4). CIPW normative mineralogy indicates a transitional composition between silica-saturated to silica-undersaturated alkaline lavas (Yoder and Tilley, 1962). The samples of this group are classified as trachybasalts (hawaiites) and basanites (mugearites), following the classification of Le Bass et al. (1986), and fall in the alkaline field of Miyashiro (1978). In the Harker diagrams (Fig. 4) Fe_2O_3, MgO, TiO_2, P_2O_5 and CaO as well as $K_2O + Na_2O$ show negative correlations with SiO_2. Data from Episode 5 plot in the high-alumina basalt field in the classification of Middlemost (1975) (Fig. 5). Variation in Pearce element ratios (Pearce, 1968; Pearce and Cann, 1973) suggests minor fractionation of plagioclase, Fe–Ti oxides, and fractionation of olivine and clinopyroxene (Fig. 6).

The lavas are enriched in Cr, Co and Ni relative to the other episodes and have high contents of Ba and Nb (Fig. 7). In the Primitive Mantle normalized multi-element plot they are enriched in the most incompatible elements such as Ba, Th and Nb and the LREE. The multi-elemental

signature is typical for intra-plate alkali basalts and OIB type lavas (Fig. 8; Sun and McDonough, 1989; Wilson, 1989; Gill, 2010).

7. Discussion

Details of the volcano-tectonic evolution of central Mexico are recorded in mafic to intermediate volcanic rocks of the SLPVF. Volcanism at the SLPVF during Eocene was calc-alkaline orogenic type and related to subduction of the Farallon plate. Mafic volcanic activity continued through the Oligocene and Miocene and ended with recent events with intra-plate characteristics. From the geological, geochronological and geochemical data presented above we recognize five volcano-tectonic episodes that represent a change from a convergent compressive environment to an extensional environment that produced calc-alkaline basaltic to andesitic and alkaline basaltic lavas and tephra that are intercalated with high-silica, rhyolitic ignimbrites, and rhyolitic-dacitic lava domes. These volcano-tectonic episodes created diverse volcanic forms that are part of the of the Sierra Madre Occidental volcanic province in the Mesa Central portion (Tristán-González et al., 2009a, 2009b; Aguillón-Robles et al., 2009). Fig. 9 summarizes the volcano-tectonic events for the Mesa Central from 60 Ma to Present showing the timing for peak activity and including important continental clastic sedimentation episodes related to basin formation by extensional tectonics. A correlation can be noticed between the five mafic-intermediate volcanic episodes described here ("andesitic and basaltic volcanism SLPVF" of Fig. 9) and the change of the tectonic setting, from subduction volcanism at >60 Ma to about 42 Ma, to transitional volcanism from 42 to 32 Ma, to intra-plate basaltic volcanism from about 32 Ma to Present. It is evident that there is a correlation between these 5 volcanic events and episodes of clastic sedimentation in basins with concrete tectonic events in the central part of Mexico (Mesa Central) with the following characteristics, a period of basin fill and subsidence at 55–42 Ma, a period of high-angle block faulting (Basin and Range faults) at 42–28 Ma, and a period of listric faulting from about 28 Ma to Present (Figs. 5, 9). Besides, in Fig. 9 are included the felsic volcanic events in this part of Mexico, such as the Ignimbrite Flare-up at 32–26 Ma and the felsic lava dome episodes at 32–28 Ma and at 24 Ma (Aguirre-Díaz and McDowell, 1991; Aguillón-Robles et al., 2009). It can be noticed in Fig. 5 that the 32–28 Ma lava dome event coincides with Episode 2 of mafic volcanism, thus indicating a bimodal volcanic stage.

The geochemical data indicate a general positive increase in the compatible elements with Mg# over time (Figs. 7, 8). The high contents of some of these elements (e.g., Ni ≈ 100 ppm; Cr > 100 ppm; Co 20–50 ppm; Fig. 7) suggest that these lavas conserved some of their original mantle values. However, the high Th, Ba, and Sr content of some samples (Fig. 10) could be interpreted as the interaction between parental magmas with basaltic andesitic composition and calc-alkaline affinity with the lower crust. The high concentrations of La, Rb and Nb suggest that these magmas interacted with the lower crust by crustal assimilation and further evolved by fractional crystallization (Figs. 6, 7). This is particularly evident in the La-La/Yb, Ba/Th-Th/Nb, and Th/Nb-La/Sm Pearce Element diagrams of Fig. 10. Episodes 1, 2 and 4 were strongly dominated by partial melting processes, whereas Episodes 3 and 5 were strongly dominated by fractionation processes (Fig. 10). These observations are consistent with the tectonic setting inferred from the Ti/Y-Zr/Y, Ni-Zr plots (Fig. 10), showing that Episode 1 corresponds to partial melting from a subduction zone setting, Episodes 2 and 3 could be characterized as transitional magmatism between subduction and intra-plate magmatism, and Episodes 4 and 5 are strongly characteristic for intra-plate basaltic magmas.

The volcano-tectonic evolution for the SLPVF is shown schematically in Fig. 11. Episode 1, and particularly Casita Blanca andesite, represents the first volcanic event in the SLPVF. The oldest unit (45.5–42.5 Ma), a calc-alkaline basaltic-andesite, was probably generated by incompatible

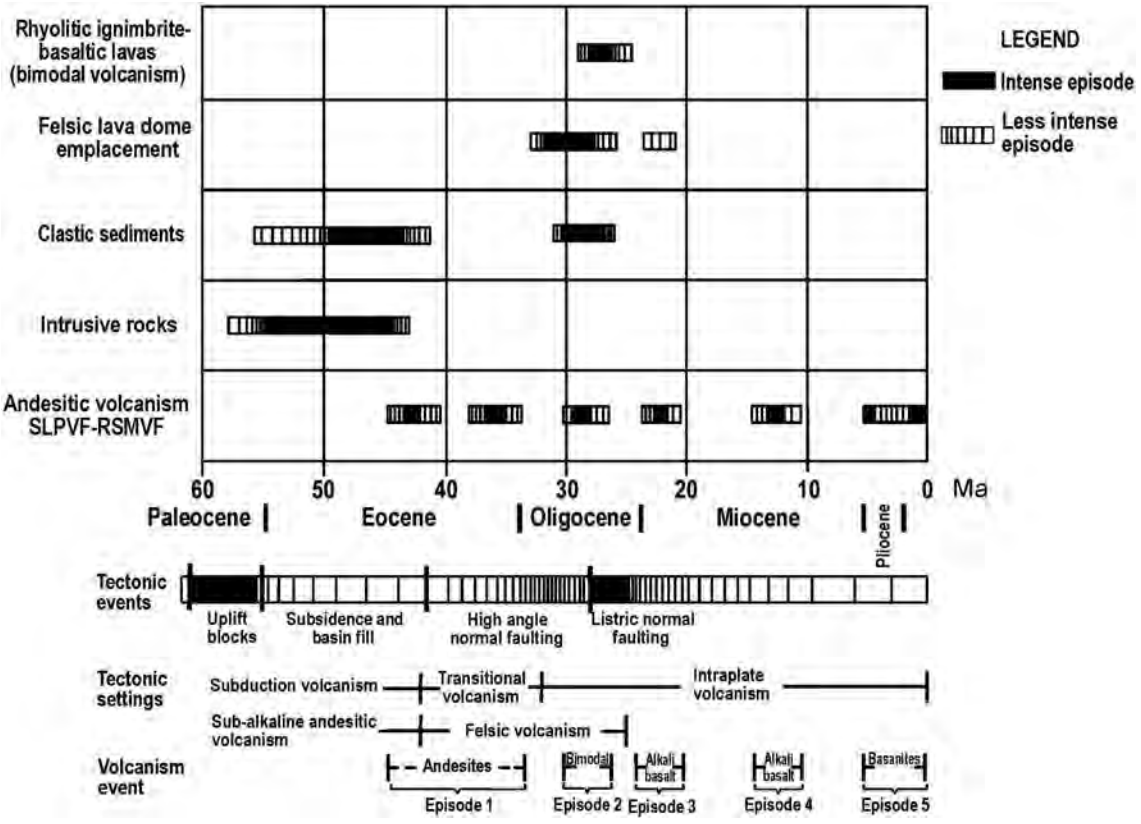

Fig. 9. Tectonic, volcanic and sedimentary events in the Mesa Central for the 60 Ma to Present interval. Modified after Aguirre-Díaz and McDowell (1991) and Tristán-González et al. (2009b).

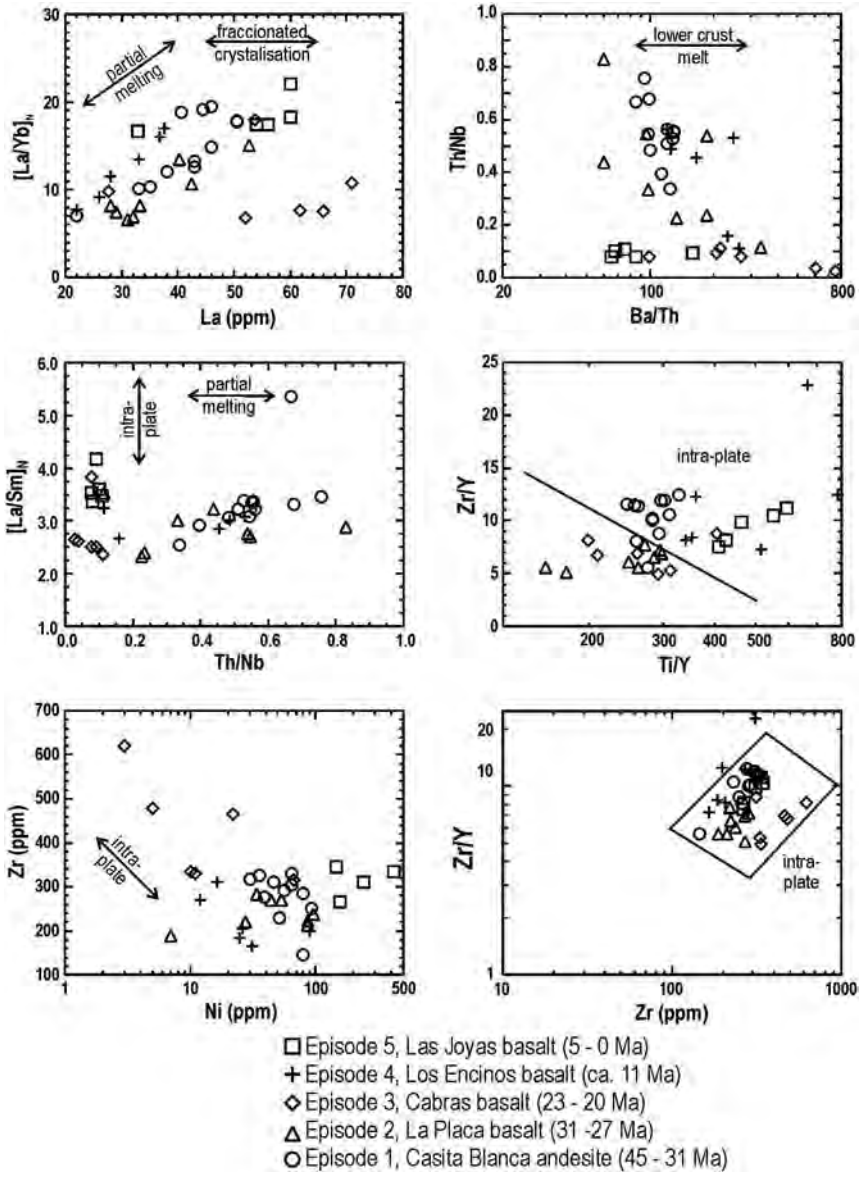

Fig. 10. Bi-element variation diagrams for representative samples of the five volcanic episodes of the SLPVF $[La/Yb]_N$ and $[La/Sm]_N$ normalized to Primitive Mantle using values of Sun and McDonough (1989).

element rich fluids derived from the asthenospheric mantle wedge that interacted with the lower crust, as has been noticed in many volcanic arcs (Gill, 1981, 2010; Wilson, 1989; Hochstaedter et al, 2000; Eiler, 2003), generating melts with low contents of Nb, Ba, Sr (Figs. 7, 8). This is confirmed with a remarkable negative anomaly of Nb in the chondrite normalized multi-element plot (Fig. 8), corresponding with the behavior of the High Field Strength Elements at subduction zone settings (Baier et al., 2007; Gill, 2010; Winter, 2010). The Oligocene andesites (36–31 Ma) show similar patterns in their multi-element plots (Fig. 8). However, it is evident that there are geochemical differences between them, such as the relative enrichment in Ba, Zr, Th, La in the Eocene andesites, and a higher Th/Nb and Zr/Y in the Oligocene andesites, which suggest a higher fusion of the crustal component from Eocene to Oligocene magmatism (Fig. 10). Thus, the Eocene lavas have a continental margin subduction setting signature and the Oligocene andesites represent a transitional stage from subduction to an intra-plate tectonic setting (Figs. 8, 9, 10, 11).

Episode 2 (29.5–28.0 Ma) volcanism shows a decrease in Ba, Th, Rb, and La, and a preservation of mantle characteristics as indicated by their high contents in Cr, Co, and Ni (Figs. 7, 8). There is a significant negative Nb anomaly associated with Episode 2 volcanic rocks as illustrated in Fig. 8. These characteristics suggest that the parental magma was derived from partial melting in the uppermost mantle that stagnated in the crust–mantle boundary with partial assimilation of the lower crust and evolved by means of slight fractional crystallization, finally producing magmas that vary in composition from basaltic-andesite to andesite (Figs. 4, 6, 7). The HREE pattern is almost horizontal confirming that the suite conserved a mantle signature (Fig. 8). The mafic magmas were coeval with high silica rhyolitic magmas, forming a bimodal volcanic event between 29.5 and 28 Ma (Tristán-González et al., 2009b; Figs. 9, 10, 11). The chemical characteristics of both basaltic andesites of Episode 2 and rhyolites of ca. 30–28 Ma (Aguillón-Robles et al., 2009) indicate an intra-plate tectonic setting in a continental extensional regime (e.g., Johnson et al., 1989; Ford et al., 2013).

Around 22 Ma there was a compositional change to mafic alkaline volcanism of Episode 3, which displays high contents of Ba, Nb, La, negative anomalies in Th and Sr, and LREE are more fractionated with respect to the HREE (Fig. 8). It conserves a mantle signature probably with assimilation of the lower crust (Figs. 10, 11). These lavas are in agreement with an intra-plate extensional continental tectonic setting

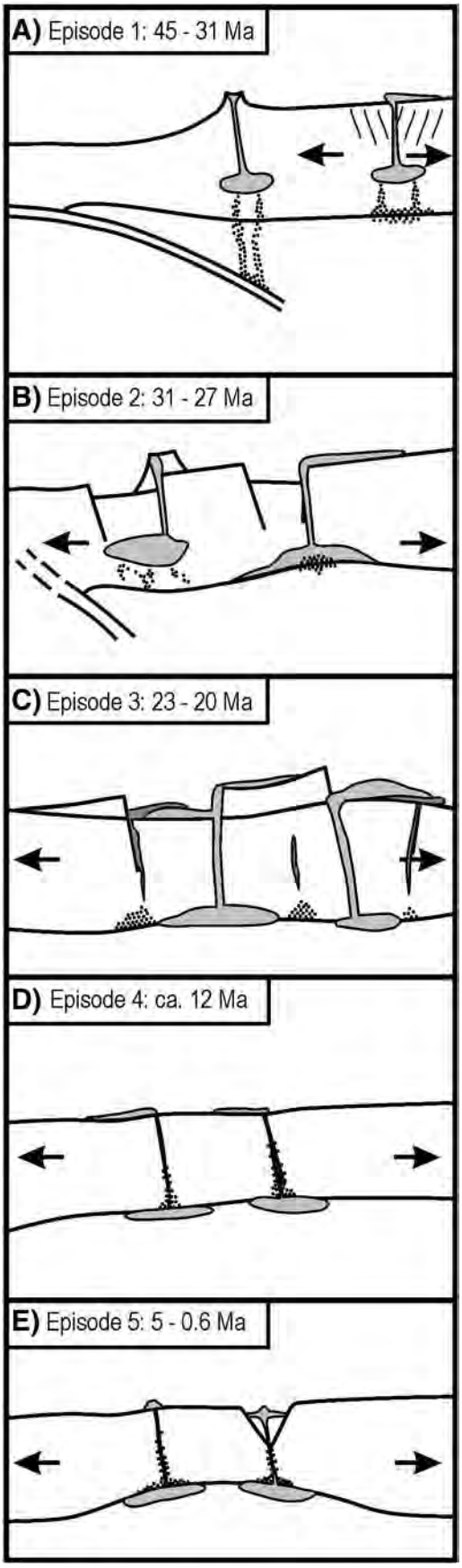

as shown in the La/Sm vs. Th/Nb and Th/Nb vs. Ba/Th plots (Wilson, 1989; Gill, 2010). Eventually, these alkaline magmas got mixed with silicic magmas forming contemporaneous trachytic lavas (Tristán-González et al., 2009b; Aguillón-Robles et al., 2009).

At 12 Ma, alkaline volcanism renewed in the SLPVF after a period of inactivity of about 10 Ma that is represented by the Los Encinos basalt of Episode 4. This suite shows enrichment of incompatible elements and a slightly negative anomaly of Nb (Figs. 7, 8), enrichment of some compatible elements (Cr, Co, Ni), and a decreasing tendency for Sr, Th, Zr and Rb, suggesting that melts were derived from partial melting at the upper mantle (Figs. 10, 11), based on the high Mg# of these basalts (60–70), fractionation of the incompatible elements with respect to the compatible elements, an enrichment of LREE and a negative tendency of HREE, and the alkaline composition. All are characteristics for intra-plate alkaline volcanism (Figs. 7, 10).

Alkaline basaltic volcanism of Episode 5, between 5 Ma and 0.6 Ma, was associated with maars and fissures controlled by regional faults oriented NNW and E–W. This volcanism is enriched in Ba and Rb and depleted in Sr, Th, Nb, Cr, Ni, and Co (Figs. 7, 8). Lavas and tephra of this event show depleted REE patterns in plots normalized to primitive mantle (Sun and McDonough, 1989; Fig. 8). Magmas were apparently derived from partial melting of the uppermost mantle and in fact there are mantle xenoliths among the erupted products at some vents. In their ascent to the surface some of this mantle derived magmas apparently stopped for a short time in the upper crust, where they had time to evolve by an AFC process; i.e., slight crustal assimilation and increasing fractional crystallization, but conserving their ultramafic signature. This is interpreted from the patterns observed in the Zr vs. Ni, La/Sm vs. Th/Nb and Th/Nb vs. Ba/Th plots (Fig. 10). Volcanism of this last episode occurred within an intra-plate continental extensional tectonic regime (Fig. 11).

8. Conclusions

- The San Luis Potosí Volcanic Field (SLPVF) of central Mexico is a mid-Tertiary volcanic area belonging to the Sierra Madre Occidental province located to the west and north of San Luis Potosí City, Mexico.
- Five volcanic episodes are identified based upon the textural and chemical characteristics of each episode, representing distinct volcano-tectonic events that took place in central Mexico from Eocene to Pleistocene.
- Episode 1 includes 45–42 Ma basaltic andesites and 36–31 Ma andesites that mark the transition from a continental margin subduction setting to an intra-plate extensional setting.
- Episode 2 includes 29.5–28 Ma basaltic andesites and andesites in bimodality with coeval high-silica rhyolitic ignimbrites that represent a peak in extension within an initiating intra-plate magmatic setting.
- Episode 3 includes 22 Ma alkaline basalts and coeval trachytes that represent a change in composition to a more typical intra-plate extensional basaltic volcanism.
- Episode 4 includes 12 Ma alkaline basalts with mantle-derived compositions interpreted as another peak in extension with contemporaneous eruption of lavas generated in continued intra-plate extensional conditions.

Fig. 11. Schematic representation of the tectono-magmatic settings that originated the five andesitic-basaltic volcanic episodes recognized in the Mesa Central of Mexico (SLPVF) between 45.5 and 0.6 Ma. A) Eocene basaltic-andesite and andesitic lavas generated in a subduction setting that evolved to intra-plate extension-related basaltic andesites by the Oligocene. B) Oligocene basaltic-andesite and andesitic lavas and coeval rhyolitic volcanism in an initial intra-plate regime. C. Early Miocene alkaline basalts and trachytic lavas within an intra-plate regime. D. Middle Miocene alkaline basaltic lavas derived from partial melting at the upper mantle in an intra-plate regime. E. Quaternary alkaline basalt associated to a mature extensional intra-plate tectonic regime.

- Episode 5 includes two sets of alkaline basalts, one at 5 Ma and the other at 1.5 to 0.6 Ma, both representing the continuation of the extensional intra-plate tectonic regime to practically present time.
- Subduction magmatism is evident in central Mexico until about 42 Ma, followed by a transitional magmatic stage subduction-intraplate from 42 to 31 Ma, to intra-plate continental extensional magmatism from about 31 to Present.

Acknowledgments

We thank the two anonymous reviewers and the editor Joan Marti for their comments and constructive criticism that helped to substantially improve this paper. We are grateful to the Instituto de Geología of the Universidad Autónoma de San Luis Potosí (UASLP) for logistical and financial support in order to carry out field work and chemical and radiometric dating analyses. The study was partly supported by the grant UNAM-PAPIIT IN-114606 to Gerardo J. Aguirre for work carried out in the Villa de Reyes graben. Erasmo Mata Martínez of the Instituto de Geología at the UASLP prepared the thin sections. We thank María Elena García-Arreola for doing some chemical analyses shown in this work.

References

Aguillón-Robles, A., Tristán-González, M., Aguirre-Díaz, G.J., Bellon, H., 2009. Syn-extensional intra-plate trachydacite-rhyolitic dome volcanism of the Mesa Central, southern Sierra Madre Occidental volcanic province, Mexico. J. Volcanol. Geotherm. Res. 187 (1–2), 33–52. http://dx.doi.org/10.1016/j.jvolgeores. 2009.08.021.

Aguillón-Robles, A., Tristán-González, M., López-Doncel, R.A., García-Arreola, M.A., Almaguer-Rodríguez, M.A., Maury, R.C., 2012. Trace elements geochemistry and origin of volcanic units from the San Luis Potosi and Rio Santa Maria volcanic fields, Mexico: the bearing of ICP-QMS data. Geofis. Int. 51 (3), 293–308.

Aguirre-Díaz, G.J., Labarthe-Hernández, G., 2003. Fissure ignimbrites: fissure-source origin for voluminous ignimbrites of the Sierra Madre Occidental and its relationship with Basin and Range faulting. Geology 31 (9), 773–776.

Aguirre-Díaz, G.J., McDowell, F.W., 1991. The volcanic section at Nazas, Durango, Mexico, and the possibility of widespread Eocene volcanism within the Sierra Madre Occidental. J. Geophys. Res. 96, 13373–13388.

Aguirre-Díaz, G.J., McDowell, F.W., 1993. Nature and timing of faulting and syn-extensional magmatism in the southern Basin and Range, central-eastern Durango, Mexico. Geol. Soc. Am. Bull. 105, 1435–1444.

Aguirre-Díaz, G.J., Labarthe-Hernández, G., Tristán-González, M., Nieto-Obregón, J., Gutiérrez-Palomares, I., 2008. Ignimbrite flare-up and graben-calderas of the Sierra Madre Occidental, Mexico. In: Gottsmann, J., Martí, J. (Eds.), Caldera Volcanism: Analysis, Modelling and Response. Developments in Volcanology, 10. Elsevier, Amsterdam. ISBN: 978-0-444-53165-0, pp. 143–180 (492 pp.).

Albretch, A., Goldstein, S.L., 2000. Effects of basement composition and age on silicic magmas across an accreted terrane–Precambrian crust boundary, Sierra Madre Occidental, Mexico. J. S. Am. Earth Sci. 13, 255–273.

Aranda-Gómez, J.J., McDowell, F.W., 1998. Paleogene extensión in the southern Basin and Range Province of Mexico: syn-depositional tilting of Eocene red beds and Oligocene volcanic rocks in the Guanajuato mining district. Int. Geol. Rev. 40, 116–134.

Aranda-Gómez, J.J., Luhr, J.F., Pier, J., 1993. Geología de volcanes cuaternarios portadores de xenolitos provenientes del manto y de la base de la corteza en el Estado de San Luis Potosí. Bol. Inst. Geol. Univ. Nac. Auton. Mex. 106, 13–22.

Aranda-Gómez, J.J., Luhr, J.F., Housh, T.B., Valdez-Moreno, G., Chávez-Cabello, G., 2005. El vulcanismo tipo intraplaca del Cenozoico tardío en el centro y norte de México: una revisión. Bol. Soc. Geol. Mex. 53 (3), 187–225.

Baier, J., Audétat, A., Keppler, H., 2007. The origin of the negative niobium tantalum anomaly in subduction zone magmas. Earth Planet. Sci. Lett. 267, 290–300.

Barboza-Gudiño, J.R., Torres-Hernández, J.R., Trsitán-González, M., 1998. The Late Triassic–Early Jurassic active continental margin of western North America in northeastern Mexico. Geofis. Int. 37 (4), 283–292.

Barboza-Gudiño, J.R., Zavala-Monsiváis, A., Venegas-Rodríguez, G., Barajas-Nigoche, L.D., 2010. Late Triassic stratigraphy and facies from northeastern Mexico: tectonic setting and provenance. Geosphere 6 (5), 621–640.

Barker, D.S., 1983. Igneous Rocks. Prentice Hall, Inc., Englewood Cliffs, NJ (417 pp.).

Bellon, H., Quoc Buu, N., Chaumont, J., Philippet, J.C., 1981. Implantation ionique d'argon dans une cible support. Application au traçage isotopique de l'argon contenu dans les minéraux et les roches. C. R. Acad. Sci. Paris 292, 977–980.

Bryan, S.E., Ferrari, L., Reiners, P.W., Allen, C.M., Petrone, C.M., Ramos-Rosique, A., Campbell, I.H., 2008. New insights into crustal contributions to large-volume rhyolite generation in the mid-Tertiary Sierra Madre Occidental Province, Mexico, revealed by U–Pb geochronology. J. Petrol. 49 (1), 47–77.

Cameron, K.L., Hanson, G.N., 1982. Rare earth element evidence concerning the origin of voluminous mid-Tertiary rhyolitic ignimbrites and related volcanic rocks, SMO, Chihuahua, Mexico. Geochim. Cosmochim. Acta 46, 1489–1503.

Cameron, K.L., Cameron, C., Babgy, W.C., Moll, E.J., Drake, R.E., 1980. Petrologic characteristics of the Mid-Tertiary volcanics suites, Chihuahua, Mexico. Geology 8, 87–91.

Cameron, K.L., Nimz, G.J., Kuentz, D., 1989. Soutern cordilleran basaltic andesite andesite suite, southern Chihuahua, Mexico: a link between Tertiary continental arc and flood basalt magmatism in North America. J. Geophys. Res. 94 (B6), 7817–7840.

Campa-Uganda, M.A., Coney, P.J., 1983. Tectono-stratigraphic terranes and mineral resource distribution in Mexico. Can. J. Earth Sci. 20, 1040–1051.

Carrillo-Bravo, J., 1971. La Plataforma Valles-San Luis Potosí. Bol. Asoc. Mex. Geol. Petrol. 13 (1–6) (113 pp.).

Carrillo-Bravo, J., 1982. Exploración Petrolera de la Cuenca Mesozoica del Centro de México. Asoc. Mex. Geol. Petrol. XXXIV (1), 21–46.

Centeno-García, E., Silva-Romo, G., 1997. Petrogenesis and tectonic evolution of central Mexico during Triassic–Jurassic time. Rev. Mex. Cienc. Geol. 14 (2), 244–260.

Clark, K.F., Damon, P.E., Schutter, S.R., Shafiqullah, M., 1979. Magmatismo en el norte de México en relación a los yacimientos metalíferos. Asociación de Ingeniero de Minas Metalalurgistas y Geólogos de México. Convención Nacional XIII, Memoria 8–57.

Cotten, J., Le Dez, A., Bau, M., Carroff, M., Maury, R., Dulski, P., Fourçade, S., Bohn, M., Brousse, R., 1995. Origin of anomalous rare-earth element and ytrium enrichments in subaereally exposed basalts: evidence from French Polynesia. Chem. Geol. 119 (1–4), 115–138.

Cox, A., Dalrymple, G.B., 1967. Statistical analysis of geomagnetic reversal data and the precision of potassium–argon dating. J. Geophys. Res. 72, 2603–2614.

Damon, P.E., Shafiqullah, M., Clark, K.F., 1981. Age trends of igneous activity in relation to metallogenesis in the southern Cordillera. Ariz. Geol. Soc. Dig. 14, 137–154.

Damon, P.E., Shafiqullah, M., Clark, K., 1983. Geochronology of the porphyry copper deposits and related mineralization in Mexico. Can. J. Earth Sci. 20 (6), 1052–1071.

Edwards, J.D., 1955. Studies of some Tertiary red conglomerates of Central Mexico. U.S. Geol. Surv. Prof. Pap. 264-H, 153–183.

Eguiluz-de Antuñano, S., Aranda-García, M., Marret, R., 2000. Tectónica de la Sierra Madre Occidental, México. Bol. Soc. Geol. Mex. LIII, 1–26.

Engebretson, D.C., Cox, A., Thompson, G.A., 1984. Correlation of plate motions with continental tectonics: Laramide to Basin–Range. Tectonics 3 (2), 115–119.

Eiler, J., 2003. Inside the subduction factory. American Geophysical Union, Washington, D.C., Geophysical monograph 138 (311 pp.).

Ford, M.T., Grunder, A.L., Duncan, R.A., 2013. Bimodal volcanism of the high lava plains and northwestern Basin and Range of Oregon: the distribution and tectonic implications of age-progressive rhyolites. In: Carlson, R.W., Fouch, M.J. (Eds.), Genesis of Continental Intraplate Magmatism — The Example from the Pacific Northwest, USA. Geochemistry Geophysics Geosystems, 14, pp. 2836–2857.

Gill, R., 1981. Orogenic Andesites and Plate Tectonics. Springer-Verlag (390 pp.).

Gill, R., 2010. Igneous Rocks and Processes: A Practical Guide. Wiley-Blackwell (428 pp.).

Guzmán, J.E., De Cserna, Z., 1963. Tectonic history of Mexico. Backbone of the Americas: Tectonic History, a Symposium. American Association Petroleum Geologists, Memoir, 2 113–129.

Harker, A., 1909. The Natural History of Igneous Rocks. Methuen, London (258 pp.).

Henry, C.D., Aranda-Gómez, J.J., 1992. The real southern Basin and Range: mid- to late Cenozoic extension in Mexico. Geology 20 (8), 701–704.

Henry, C.D., Fredrikson, G., 1987. Geology of part of southern Sinaloa, Mexico adjacent to the Gulf of California. Geological Society of America Map and Chart Series MCH063 (14 pp.).

Hochstaedter, A.G., Gill, J.B., Taylor, B., Ishizuka, O., Yuasa, M., Morita, S., 2000. Across-arc geochemical trends in the Izu-Bonin arc: constraints on source composition and mantle melting. J. Geophys. Res. 105, 495–512.

Hoppe, M., Barboza-Gudiño, J.R., Schulz, H.M., 2002. Late Triassic submarine fan in northwestern San Luis Potosí, México—lithology, facies and diagenesis. N. Jb. Geol. Paläont. 2002, 705–724.

Humphreys, E., 2009. Relation of flat subduction to magmatism and deformation in the western United States. In: Mahlburg Kay, Suzanne, Ramos, Víctor A., Dickinson, William R. (Eds.), Backbone of the Americas: Shallow Subduction, Plateau Uplift, and Ridge and Terrane Collision. Geological Society of America Memoirs, 204, pp. 85–98 (Geological Society of America books, Boulder, Colorado).

Idier, C., 2003. Caractéristiques des évènements magmatiques Eocènes-Oligocènes et Plio-Quaternaires du champ volcanique de San Luis Potosi (Mexique). Ecole Doctorale des Sciences de la Mer, Université de Bretagne Occidentale ([Mémoire de Licence], 55 pp.).

Johnson, R.W., Knutson, J., Taylor, R.S., 1989. Intraplate Volcanism in Eastern Australia and New Zealand. Australian Academy of Science. Cambridge University Press (408 pp.).

Labarthe-Hernández, G., Jiménez-López, L.S., 1992. Características físicas y estructura de lavas e ignimbrita riolíticas en la Sierra de San Miguelito. S.L.P. Instituto de Geología, 114. Universidad Autónoma de San Luis Potosí, Foll. Téc.(31 p.).

Labarthe-Hernández, G., Tristán-González, M., Aranda-Gómez, J.J., 1982. Revisión estratigráfica del Cenozoico de la parte central del Estado de San Luis Potosí. Folleto Técnico (Open File Report), 85. Universidad Autónoma de San Luis Potosí, Instituto de Geología (205 pp.).

Labarthe-Hernández, G., Tristán-González, M., Aguillón-Robles, A., 1984. Cartografía geológica 1:50,000 Salitrera, S.L.P. Universidad Autónoma de San Luis Potosí, Instituto de Geología, Folleto Técnico (Open File Report) 94, 85 pp.

Labarthe-Hernández, G., Aguillón Robles, A., Tristán-González, M., Jiménez-López, L.S., Romero, A., 1989. Cartografía geológica 1:50,000 de las Hoja El Refugio y Mineral El Rialito. Instituto de Geología, 112. Universidad Autónoma de San Luis Potosí, Foll. Téc.(76 p.).

Labarthe-Hernández, G., Sánchez-Pérez, M., Vázquez-Guillén, M., 1999. Mapa geológico del Volcán Atotonilco, S.L.P., México. Folleto Técnico (Open File Report), 125. Universidad Autónoma de San Luis Potosí, Instituto de Geología (19 pp.).

Le Bas, M.J., Le Maitre, R.W., Streckeisen, A., Zanettin, B., 1986. A chemical classification of volcanic rocks based on the total alkali–silica diagram. J. Petrol. 27 (3), 745–750.

Livaccari, R.F., Burke, K., Şengör, A.M.C., 1981. Was the Laramide orogeny related to subduction of an oceanic plateau? Nature 289, 276–279.

Luhr, J.F., Pier, J.G., Aranda-Gómez, J.J., Podosek, F., 1995. Crustal contamination in early Basin-and-Range hawaiites of the Los Encinos volcanic field, central México. Contrib. Mineral. Petrol. 118 (4), 321–339.
Mahood, G.A., Drake, R.E., 1982. K–Ar dating young rhyolitic rocks: a case study of the Sierra La Primavera, Jalisco, Mexico. Geol. Soc. Am. Bull. 93 (12), 1232–1241.
Martínez-Esparza, G., 2004. Geoquímica de las rocas andesíticas del Campo Volcánico de San Luis Potosí. Universidad Autónoma de San Luis Potosí, Facultad de Ingeniería (Tesis de Licenciatura, 66 pp.).
McDowell, F.W., Clabaugh, S.E., 1979. Ignimbrites of the Sierra Madre Occidental and their relation to the tectonic history of western Mexico. Geol. Soc. Am. Spec. Pap. 180, 113–124.
McDowell, F.W., Keiser, 1977. Timing of mid-Tertiary volcanism in the Sierra Madre Occidental between Durango City and Mazatlan, Mexico. Geol. Soc. Am. Bull. 88 (10), 1479–1486.
McDowell, F.W., Mauger, R.L., Walker, N.W., 1989. Geochronology of Cretaceous–Tertiary magmatic activity in central Chihuahua, Mexico, continental magmatism. Bull. New Mex. Bur. Min. Miner. Resour. 131, 181.
McDowell, F.W., Roldán-Quintana, J., Connelly, J.N., 2001. Duration of late Cretaceous–early Tertiary magmatism in east-central Sonora, Mexico. Geol. Soc. Am. Bull. 113 (4), 521–531.
Middlemost, E.A.K., 1975. The basalt clan. Earth-Sci. Rev. 11 (4), 337–364.
Miyashiro, A., 1978. Nature of alkalic volcanic rocks series. Contrib. Mineral. Petrol. 66 (1), 91–104.
Molnar, P., Atwater, T., 1978. Interarc spreading and Cordilleran tectonics as alternates related to the age of subducted oceanic lithosphere. Earth Planet. Sci. Lett. 41 (3), 330–340.
Nemeth, K.E., 1976. Petrography of the Lower Volcanic Group Tayoltita–San Dimas District, Durango, Mexico. University of Texas at Austin, Texas (M.A. Thesis, 141 pp.).
Pearce, T.H., 1968. A contribution to the theory of variation diagrams. Contrib. Mineral. Petrol. 19 (2), 142–157.
Pearce, J.A., Cann, J.R., 1973. Tectonic setting of basic volcanic rocks determined using trace element analyses. Earth Planet. Sci. Lett. 19 (2), 290–300.
Peccerillo, A., Taylor, S.R., 1976. Geochemistry of Eocene calc-alkaline volcanic rocks from the Kastamonu area, northern Turkey. Contrib. Mineral. Petrol. 58 (1), 63–81.
Rodríguez-Ríos, R., Torres-Aguilera, J.M., 2009. Petrología y Geoquímica del Vulcanismo Bimodal Oligocénico en el Campo Volcánico de San Luis Potosí (México). Rev. Mex. Cienc. Geol. 26 (3), 658–673.
Roldán-Quintana, J., 1991. Geology and chemical composition of El Jaralito and Aconchi batholiths in east-central Sonora. In: Pérez-Segura, E., Jacques-Ayala, C. (Eds.), Studies of Sonoran Geology. Geological Society of America, Special Paper, 254, pp. 19–36.
Sánchez-García, A.C., 2009. Descripción de posibles fallas sismogénicas regionales en la Zona Media del Estado de San Luis Potosí, SLP. Universidad Autónoma de San Luis Potosí, Facultad de Ingeniería ([Tesis Licenciatura], 80 pp.).
Saucedo-Girón, R., Gómez-Villa, W., Cerda-Díaz, J.H., Torres-Hernández, J.R., Macías, J.L., 2011. Estudio estratigráfico del Maar Joya Honda, San Luis potosí. Unión Geofísica Mexicana, Reunión Anual. GEOS, 31(1) 132.
Shaaf, P., Heinrich, W., Besch, T., 1994. Composition and Sm–Nd isotopic data of the lower crust beneath San Luis Potosí, central Mexico: evidence from a granulite-facies xenolith suite. Chem. Geol. 118 (1–4), 63–84.
Steiger, R.H., Jäger, E., 1977. Subcommission on geochronology: convention on the use of decay constants in geo- and cosmochronology. Earth Planet. Sci. Lett. 36 (3), 359–362.
Stewart, J.H., 1998. Regional characteristics, tilt domains, and extensional history of the late Cenozoic Basin and Range province, western North America. Geol. Soc. Am. Spec. Pap. 323, 47–74.
Sun, S.S., McDonough, W.F., 1989. Chemical and isotopic systematics of oceanic basalt: implications for mantle compositions and processes. In: Saunders, A.D., Norry, M.J. (Eds.), Magmatism in the Ocean Basin. Geological Society of London Special Publication, 42, pp. 313–345.
Thornton, C.P., Tuttle, O.F., 1960. Chemistry of igneous rocks. I. Differentiation index. Am. J. Sci. 258 (9), 664–684.
Torres-Aguilera, J.M., 2005. Caracterización petrográfica y geoquímica del vulcanismo bimodal en el semigraben de Bledos, en el Campo Volcánico de San Luis Potosí: San Luis Potosí, México. Universidad Autónoma de San Luis Potosí, Facultad de Ingeniería ([Tesis de Maestría], 159 pp.).
Torres-Hernández, J.R., Labarthe-Hernández, G., Aguillón-Robles, A., Gómez-Anguiano, M., Mata-Segura, J.L., 2006. The pyroclastic dikes of San Luis Potosí volcanic field: implications on the emplacement of Panalillo ignimbrite. Geofis. Int. 45 (4), 243–253.
Tristán-González, M., 1986. Estratigrafía y tectónica del Graben de Villa de reyes, en los estados de San Luis Potosí y Guanajuato, México. Folleto Técnico (Open File Report), 107. Universidad Autónoma de San Luis Potosí, Instituto de Geología (91 pp.).
Tristán-González, M., 2008. Evolución tectono-magmática durante el Paleógeno en la porción sur-oriental de la Mesa Central. Universidad Nacional Autónoma de México, Centro de Geociencias ([Tesis de Doctorado], 207 pp.).
Tristán-González, M., Labarthe-Hernández, G., 1979. Cartografía geológica Hoja Tepetate, S.L.P. Folleto Técnico (Open File Report), 66. Universidad Autónoma de San Luis Potosí, Instituto de Geología y Metalurgia (31 pp.).
Tristán-González, M., Labarthe-Hernández, G., Aguillón-Robles, A., Torres-Hernández, J.R., Aguirre-Díaz, J.G., 2006. Diques Piroclásticos en fallas de extensión alimentadores de ignimbritas, en el occidente de Campo Volcánico del Río Santa María, S.L.P Unión Geofísica Mexicana, Reunión Anual. GEOS, 26(1) 163.
Tristán-González, M., Aguirre-Díaz, J.G., Labarthe-Hernández, G., Aguillón-Robles, A., 2008. Tectono-volcanic control of fissure type vents for the 28 Ma Panalillo ignimbrite in the Villa de Reyes Graben, San Luis Potosí, Mexico: Workshop Calderas, Conf. Series. Earth Environ. Sci. 3. http://dx.doi.org/10.1088/1755-1307/3/1/012026.
Tristán-González, M., Aguillón-Robles, A., Barboza-Gudiño, J.R., Torres-Hernández, J.R., Bellon, H., López-Doncel, R.A., Rodríguez-Ríos, R., Labarthe-Hernández, G., 2009a. Geocronología y distribución espacial del Campo Volcánico de San Luis Potosí. Bol. Soc. Geol. Mex. 61 (3), 287–303.
Tristán-González, M., Aguirre-Díaz, G.J., Labarthe-Hernández, G., Torres-Hernández, J.J., Bellon, H., 2009b. Post-Laramide and pre-Basin and Range deformation and implications for Paleogene (55–25 Ma) volcanism in central Mexico: a geological basis for a volcano-tectonic stress model. Tectonophysics 471 (1–2), 136–152. http://dx.doi.org/10.1016/j.tecto.2008.12.021.
Verma, S.P., Sotelo Rodríguez, Z.T., Torres Alvarado, I.S., 2002. SINCLAS: Standard Igneous Norm and Volcanic Rock Classification System. Comput. Geosci. 28 (5), 711–715.
Wilkinson, J.F.G., 1982. The genesis of mid-ocean ridge basalt. Earth-Sci. Rev. 18 (1), 1–57.
Wilson, M., 1989. Igneous Petrogenesis. A Global Tectonic Approach. Unwin Hyman, London (466 pp.).
Winter, J.D., 2010. Principles of Igneous and Metamorphic Petrology. Prentice Hall (720 pp.).
Yoder, H.S., Tilley, C.E., 1962. Origin of basalt magmas: an experimental study of natural and synthetic rock system. J. Petrol. 3 (3), 342–532.
Zavala-Monsiváis, A., Barboza-Gudiño, J.R., Velasco-Tapia, F., García-Arreola, M.E., 2012. Sucesión volcánica Jurásica en el área de Charcas, San Luis Potosí: Contribución al entendimiento del Arco Nazas en el noreste de México. Bol. Soc. Geol. Mex. 64 (3), 277–293.